

# Lost at Sea: Identifying the Post-Depositional Alteration of Amphorae in Ancient Shipwrecks

Miše, M.<sup>1</sup>, Quinn, S. P.<sup>1</sup> and Glascock, M. D.<sup>2</sup>

<sup>1</sup> Institute of Archaeology, University College London, 31-34 Gordon Square, London, WC1H0PY. ([mmaja17@yahoo.co.uk](mailto:mmaja17@yahoo.co.uk))

<sup>2</sup> Archaeometry Laboratory, University of Missouri Research Reactor, 1513 Research Park Drive, Columbia, MO 65211, USA

## Abstract

The present paper sheds new light on the alteration of archaeological ceramics buried in marine environments by analysing in detail a large dataset of Hellenistic and Late Roman Republican transport amphorae from 15 sites along the well-known ancient maritime trade route off the Dalmatian coast in southern Croatia. These include amphorae from shipwrecks, kiln sites and settlements. Ceramic petrography and instrumental neutron activation analysis (INAA) have been used to compare sherds of the same fabric and origin, but recovered from both shipwrecks and terrestrial sites and were therefore exposed to different burial environments. The integration of both methods permitted the identification of differential microstructural and geochemical alteration of the amphorae under the sea relative to those found on land. By applying principal components analysis and test statistics, we have detected enrichment of As, Ca, Na, Sb, Sr and U and depletion of Ba, Cs, K and Rb in amphorae from the marine environment, relative to those buried on land. The implications of the study are discussed in terms of the provenance determination of amphorae from submerged environments and the reconstruction of ancient maritime trade routes.

**Keywords:** pottery, transport amphorae, ceramic petrography, geochemistry, test statistics, alteration; shipwrecks; seawater; provenance determination; maritime trade

## Introduction

Studies of ancient Mediterranean economy and trade have largely relied on the distribution of inorganic archaeological artefacts such as metals, glass and most crucially, pottery. From as early as the Bronze Age, as evidenced by the Canaanite and large Cypriot jars found within the 14<sup>th</sup> c. BC Uluburun shipwreck off the coast of the Turkey, until Late Antiquity ceramic containers were used to transport goods over significant distances (Bevan 2014). Amphorae, a common type of transport vessel used in the Mediterranean during Graeco-Roman periods and served as packaging for the transport and trade of olive oil, wine and fish sauce (Horden and Purcell 2000; Bevan 2014), in the same way that modern food stuffs are distributed in standardised plastic or glass containers. Whilst the contents of ancient amphorae have been consumed or perished in the intervening millennia, the vessels themselves remain, often as broken sherds, at archaeological sites. Here they represent a valuable record of the commerce and other economic activity that took place in the ancient Mediterranean.

The submerged remains of ships that sunk mid voyage, laden with cargo, are particularly important indicators of past trade activities. The large number of shipwrecks dated from the Late Classical to Early Roman Imperial period (late 5<sup>th</sup> c. BC to 1<sup>st</sup> c. AD) in the Mediterranean basin serve as evidence that a complex web of commercial connections (Parker 1992; Gibbins 2001) existed during this period of economic growth (Archibald 2013). Archaeologists have sought to untangle this by interpreting the production locations of amphorae and other types of

transport vessels using both typological and scientific data (e.g. Peacock 1977; Picon and Empereur 1986; Whitbread 1995). By mapping the distribution of specific vessel shapes on land and within shipwrecks, it is possible to reconstruct the direction, distance and intensity of ancient trade routes.

Certain amphorae types are known to be characteristic of particular workshops or geographical regions and were used to transport specific types of commodities, such as Mendaian amphorae produced in Chalkidian polis in northern Greece (Papadopoulos and Paspalas 1999) and amphorae from on the Aegean islands of Chios and Thasos, both of which contained wine (Horden and Purcell 2001: 225). However, similar vessel shapes are known to have been produced by several workshops, for example Type B amphorae. It was previously hypothesised that these were made in Corinth and the Corinthian colony on Corfu from 4<sup>th</sup> till late 3<sup>rd</sup> c. BC (Koehler 1979 and 1981; Whitbread 1995). Nevertheless, studies from southern Italy have shown that identical forms were also produced in Greek colonies in southern Italy and Sicily (Barone *et al.* 2004a; Barone *et al.* 2014b; Barone *et al.* 2011; Swift 2011). From the late 5<sup>th</sup> c. BC, certain workshops begun to stamp the handles of their amphorae, as an explicit statement of their provenance (Bevan 2014) or the names of their producers (Tzochev 2009). However, the vast majority of transport vessels were not labelled in this way.

Both shape and epigraphic information are not always available from small fragmented sherds and compositional analysis of the clay paste of transport amphorae via ceramic petrography and geochemistry has therefore been widely applied to determine the production location or provenance of amphorae and other types of ancient transport vessels in Western Mediterranean (Martínez Ferreras *et al.* 2007; Martínez Ferreras *et al.* 2015; Fantuzzi *et al.* 2016; Fantuzzi *et al.* 2019; Moreno Megías *et al.* 2020), in Central Mediterranean in Italy (Barra Bagnasco *et al.* 2001; Olcese 2007; Pecchioni *et al.* 2007; Swift 2011; Miriello *et al.* 2015; Carratoni *et al.* 2016) and Sicily (Barone *et al.* 2004a; Barone *et al.* 2004b; Barone *et al.* 2005; Barone *et al.* 2011; Barone *et al.* 2014), Adriatic (Machut *et al.* 2015; Ceccarelli *et al.* 2016; Maritan *et al.* 2019; Miše *et al.* 2019) and Aegean region (Hein *et al.* 2008; Day *et al.* 2011; Hein 2014). The characterisation of wasters from known kiln sites has permitted the establishment of ‘reference groups’ or ‘control groups’, that can be directly compared to sherds of transport vessels found on land and under the sea, in order to detect compositional matches that are suggestive of their origins (e.g. Martínez Ferreras *et al.* 2015; Finocchiaro *et al.* 2018).

Bulk instrumental geochemistry has been widely applied to ancient amphorae in the study of ancient shipping and trade within the Mediterranean basin, via methods such as instrumental neutron activation analysis (INAA), X-ray fluorescence (XRF) and inductively coupled plasma mass spectrometry (ICP-MS) (e. g. Farnsworth *et al.* 1977; Barra Bagnasco *et al.* 2001; Barone *et al.* 2004a; Barone *et al.* 2004b; Hein *et al.* 2008; Fantuzzi *et al.* 2019; Moreno Megías *et al.* 2020). In most such studies, quantitative multivariate chemical data is explored and classified statistically in order to identify compositional groups of known origin and match samples from different sites. However, the differential preservation of ceramic material under the sea compared to on land (Nieto and Picon 1986; Buxeda I Garrigós *et al.* 2005) (Fig. 1) may mean that pottery made from the same raw materials and technology at the same production site may no longer match chemically. Temperature cycles, freezing, load pressure, groundwater composition, acidity, saturation and redox conditions can result in the alteration of pottery during burial (Nieto and Picon 1986; Golitko *et al.* 2012; Secco *et al.* 2011). The porosity of low-fired pottery is such that fluids can pass into and through them, altering their composition by dissolving, precipitating and redistributing soluble minerals and chemicals such as calcite, gypsum and phosphate. While the post-depositional transformation of pottery from terrestrial

sites has been fairly well studied (Freestone 2001; Schwedt *et al.* 2004; Schneider 2016; Maritan 2020) and criteria have been proposed to identify potential alteration phenomena in thin sections (Cau Ontiveros *et al.* 2002; Quinn 2013: 204–210), relatively less attention has been given to the fate of artefacts buried in marine environments. Transport amphorae in shipwrecks and pottery from submerged marine sites can potentially be subjected to more intense alteration than those on land, due to the higher concentration of dissolved ions in seawater and the greater length of time that sherds are exposed to it.



Figure 1. Hellenistic Amphorae from Dalmatian sites, A. Graeco-Italic amphorae from Pharos on the island of Hvar, B. Type B from Gnjilna shipwreck near the island of Vis show different preservations of amphorae buried on land and seabed

Some geochemical studies on Mediterranean shipwrecks have identified possible elements that could have been altered within submerged amphorae, including Ca, Cs, K, Mg, Na, Rb and Sr (e.g. Nieto and Picon 1986; Pradell *et al.* 1996; Taylor *et al.* 1997; Buxeda I Garrigós *et al.* 2005; Martínez Ferreras *et al.* 2015), and laboratory experiments have been conducted on ceramic briquettes soaked in seawater (Montana *et al.* 2014). However, little or no direct comparisons have been made between sherds from the same source buried in both marine and terrestrial environments. With the exception of Martínez Ferreras *et al.* (2015), most studies have applied geochemistry without the supporting mineralogical and microstructural information offered by ceramic petrography. The present paper attempts to fill this gap using a large dataset of Hellenistic and Late Roman Republican transport amphorae from numerous sites along the well-known ancient maritime trade route of the Dalmatian coast of southern Croatia (Fig. 2). This includes production debris from known kiln sites, submerged amphorae from multiple shipwrecks and amphorae from consumption contexts on land. Ceramic petrography has been used to detect compositional groups of common origin and identify evidence for post-depositional alteration. The geochemical correspondence and dissimilarity between the representatives of each fabric recovered from marine and terrestrial environments has then been assessed using INAA and applying multivariate and test statistics. In this way, it has been possible to highlight those elements that have been enriched or depleted in the amphorae from shipwrecks, relative to those found on land and thus better understand their taphonomic alteration. The findings of the study are discussed in terms of the provenance determination of amphorae from submerged environments and the reconstruction of ancient maritime trade.

## Materials and Methods

A total of 264 amphorae sherds were selected from 15 different archaeological sites along the Dalmatian coast of southern Croatia in the Adriatic Sea (Fig. 2; Table 1), which was known to

be a maritime trade route in Hellenistic and Late Roman Republican times. These include two kiln sites and five shipwrecks, one associated with the kiln and local production on the island of Issa (Cambi 1972 and 1989), plus one harbour's land facilities site at Resnik or ancient Siculi, six Iron Age indigenous settlements where amphorae were deposited after the consumption of their contents and two sanctuaries with amphorae deposits associated with wine sacrifices. The selected samples belong to the most common types of amphorae circulating the Adriatic-Ionian region between 4<sup>th</sup>–1<sup>st</sup> c. BC, namely Corinthian A', Corinthian Type B, Greco-Italic and Lamboglia 2 amphorae (Table 1). All sherds form part of an on-going study of maritime connections, trade and the economy of the Adriatic region in pre-Roman times.

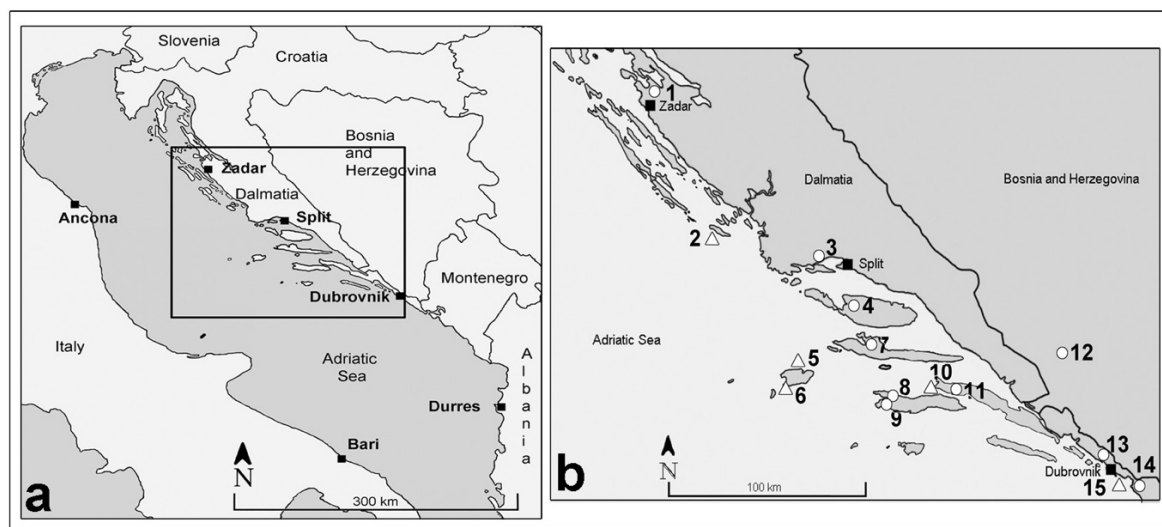


Figure 2. A) Adriatic region with Dalmatia region, southern Croatia, B) Location of amphorae containing sites in Dalmatia analysed in this study. 1. Iron Age settlement of Zemunik; 2. Žirje shipwreck; 3. Late Hellenistic/Late Roman Republican harbour of Resnik/Siculi; 4. Iron Age settlement of Vičja luka/Rat on the island of Brač; 5–6. Vela Svitnja bay Gnjilna shipwrecks, both near the island of Vis; 7. Greek city of Pharos on the island of Hvar; 8–9. Iron Age settlements of Kopila and Stine, both on the island of Korčula; 10. Polačišće shipwreck in the Pelješac channel; 11. Sanctuary of Nakovana Cave on the Pelješac peninsula; 12. Iron Age settlement of Crveni Grm in southern Herzegovina; 13. Sanctuary of Vilina Cave; 14. Iron Age settlement of Sokol fortress; 15. Supetar –Cavtat shipwreck near Dubrovnik. See Table 1 for numbers of amphorae sherds sampled per site.

Visual observations were made of the preservation of the amphorae in terms of surface encrustation, as well as colour variation on a fresh break. All samples were then thin sectioned to 30 µm in a vertical orientation (Whitbread 1995: 415) and observations were made of possible post-depositional alteration seen in thin section under the polarising light microscope at magnifications of x25–200, using established criteria (Cau Ontiveros *et al.* 2002; Quinn 2013: 204–210). The 264 thin sections of amphorae were classified into petrographic fabrics or recipes of common raw materials and technology (Quinn 2013: 73–102). Stylistically similar amphorae from terrestrial and marine sites that share the same paste recipe were assumed to have a common provenance.

The bulk geochemical composition of the amphorae sherds was characterised via INAA at the Missouri University Research Reactor (MURR) Due to possible contamination of sherds in the marine environment, c. 1 cm<sup>2</sup> of the samples surface were cleaned with a silicon carbide drill

bit before the core of samples were crushed into a powder. Approximately 150 mg of powder was placed in a high-density polyethylene vial and used for short irradiations, and c. 200 mg was transferred to a high-purity quartz vial for long irradiations. The amphorae powders were analysed along with NIST certified standard reference materials SRM-1633b (Coal Fly Ash), SRM-688 (Basalt Rock), SRM-278 (Obsidian Rock) and an in-house standard (New Ohio Red Clay; Glascock 1992) for calibration and quality control purposes. The samples were exposed to two irradiations and three gamma rays counts (Glascock 1992), resulting in the qualification of a total of 33 elements (Al, As, Ba, Ca, Ce, Co, Cr, Cs, Dy, Eu, Fe, Hf, K, La, Lu, Mn, Na, Nd, Ni, Rb, Sb, Sc, Sm, Sr, Ta, Tb, Ti, Th, U, V, Yb, Zn, and Zr).

*Table 1. Details of archaeological sites and amphorae from the Dalmatian region analysed in this study. G-I = Graeco-Italic (G-I); L2 = Lamboglia 2.*

<b>SITE</b>	<b>ID</b>	<b>TYPE OF SITE</b>	<b>TYPE OF AMPHORAE</b>	<b>NUMBER</b>
<b>ISSA</b>	VS	shipwreck/production site	L2	35
<b>PHAROS</b>	SG	production site	Corinth A' and Type B	30
<b>RESNIK/SICULI</b>	RES	harbour (land facilities)	L2	35
<b>RAT VIČJA LUKA</b>	RAT	Iron Age settlement	Corinth A' and Type B	8
<b>NAKOVANA CAVE</b>	NAK	sanctuary	L2	20
<b>VILINA CAVE</b>	VIC	sanctuary	Type B	35
<b>STINE</b>	STN	Iron Age settlement	Corinth A' and Type B, G-I	2
<b>KOPILA</b>	KOP	Iron Age settlement	Corinth A' and Type B, G-I	2
<b>CRVENI GRM (BH)</b>	CG	Iron Age settlement	Type B	6
<b>ZEMUNIK</b>	ZEM	Iron Age settlement	Type B	3
<b>SOKOL FORTRESS</b>	SOK	Iron Age settlement	Type B	15
<b>SUPETAR-CAVTAT</b>	SUP	shipwreck	Type B	15
<b>POLAČIŠĆE BAY</b>	POL	shipwreck	L2	23
<b>ŽIRJE</b>	ZIR	shipwreck	Type B	25
<b>GNJILNA</b>	GN	shipwreck	Type B	10
			<b>Total</b>	<b>264</b>

The structure of the bulk geochemical data was investigated using multivariate statistics and test statistics to compare data from different environments, namely the marine and terrestrial, using the software package R-studio. Principal components analysis (PCA) was used to reveal compositional patterning and determine the elements that were responsible for the detected groups. The data was transformed using centred log ratio transformation prior to PCA. Various comparisons were made between the geochemical patterning in the dataset and both the petrographic classification of the sherds and the environment in which they were buried (terrestrial or marine).

The degree of chemical variability within the sherds of selected large petrographic fabrics was calculated for each the 33 analysed elements, in order to identify those which differ the most and may therefore have been preferentially altered in the sea compared to on land. The samples of the same fabric group, recovered from different environments, were then subjected to test statistics. An F-test was used to compare to compare variance between samples from a marine and terrestrial environment, and a t-test was used to compare the mean values between samples from these two environments. Those elements that were suspected to have been enriched or depleted, within sherds buried in the sea bed compared to those found on land, were then removed before re-running PCA on the dataset, to see the effect this had on the geochemical correspondence of petrographically related samples from the two environments. Finally, the processes that could have been responsible for the alteration of the amphorae from marine and terrestrial contexts were considered using previous studies on the post-depositional alteration of pottery.

## **Results**

### **Petrographic Classification**

Several distinct petrographic fabrics as well as numerous unique sherds were detected among the 264 ceramic samples in thin section. Four of the petrographic fabrics, each of which contain different types of amphorae, consist of sherds recovered from both terrestrial sites and shipwrecks. Other fabric groups in our Dalmatian amphorae dataset, as well a detailed reconstruction of trade routes, will be presented separately.

Fabric 1 is the largest with 45 sherds of Lamboglia 2 amphorae from two terrestrial sites and 49 amphorae from two shipwrecks. It is characterised in thin section by silt-sized inclusions of abundant quartz, clay pellets, biotite mica, chert and foraminifera microfossils, plus rare plagioclase feldspar and muscovite mica, in a light coloured calcareous clay matrix (Fig. 3A). Fabric 2 consists of 50 Corinthian Type B amphorae from five terrestrial consumption sites, and six amphorae from two shipwrecks. It is characterised by well-sorted inclusions of abundant quartz, clay pellets, muscovite and biotite mica and chert in a calcareous clay matrix (Fig. 3B). Eight of also Corinthian Type B amphorae from four terrestrial consumption sites and seven amphorae from one shipwrecks form Fabric 3. This contains bimodal inclusions of mono- and polycrystalline quartz and biotite mica, as well as less abundant plagioclase feldspar, amphibole, clay pellets and chert in a dark red non-calcareous clay matrix (Fig. 3C). Finally, Fabric 4 consists of two Corinthian A' amphorae, one amphorae from a shipwreck and one from a terrestrial site. It contains larger inclusions of mudstone and rarely chert and finer inclusions are quartz, biotite mica and plagioclase feldspar (Fig. 3D).

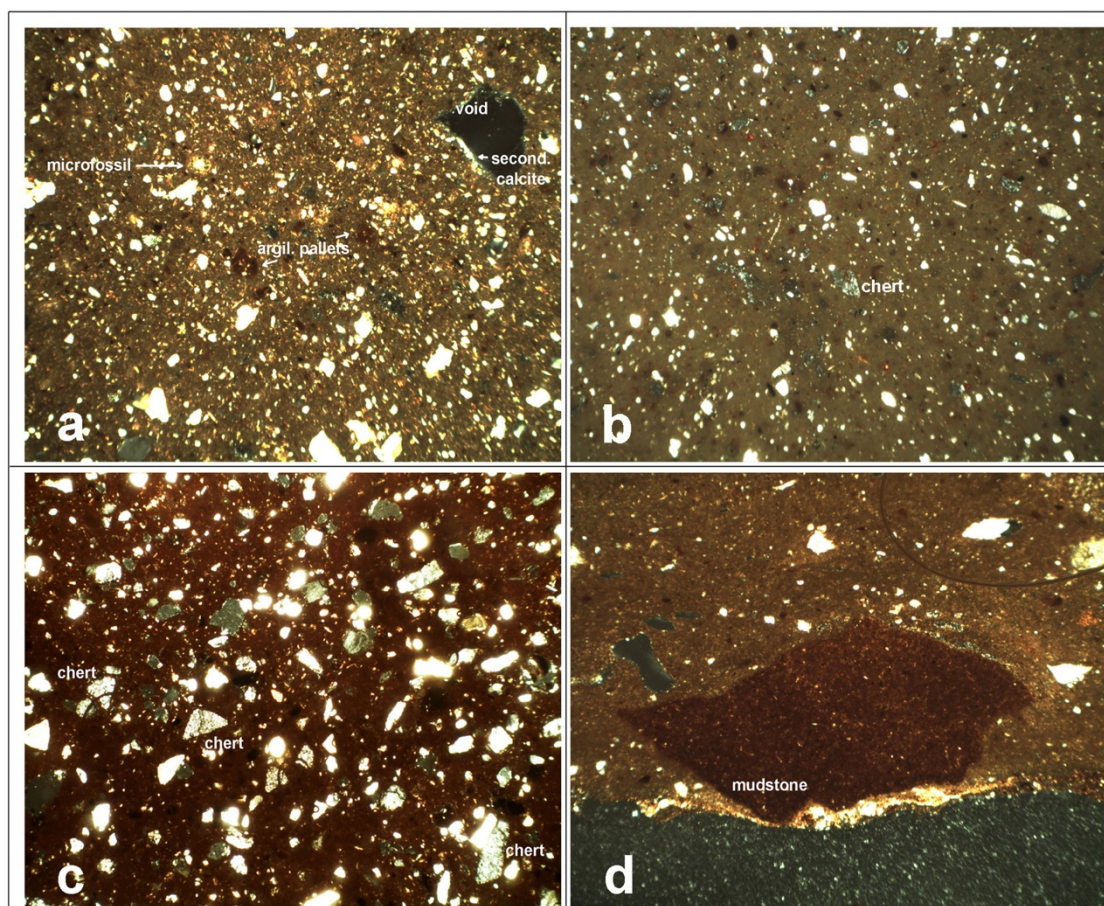
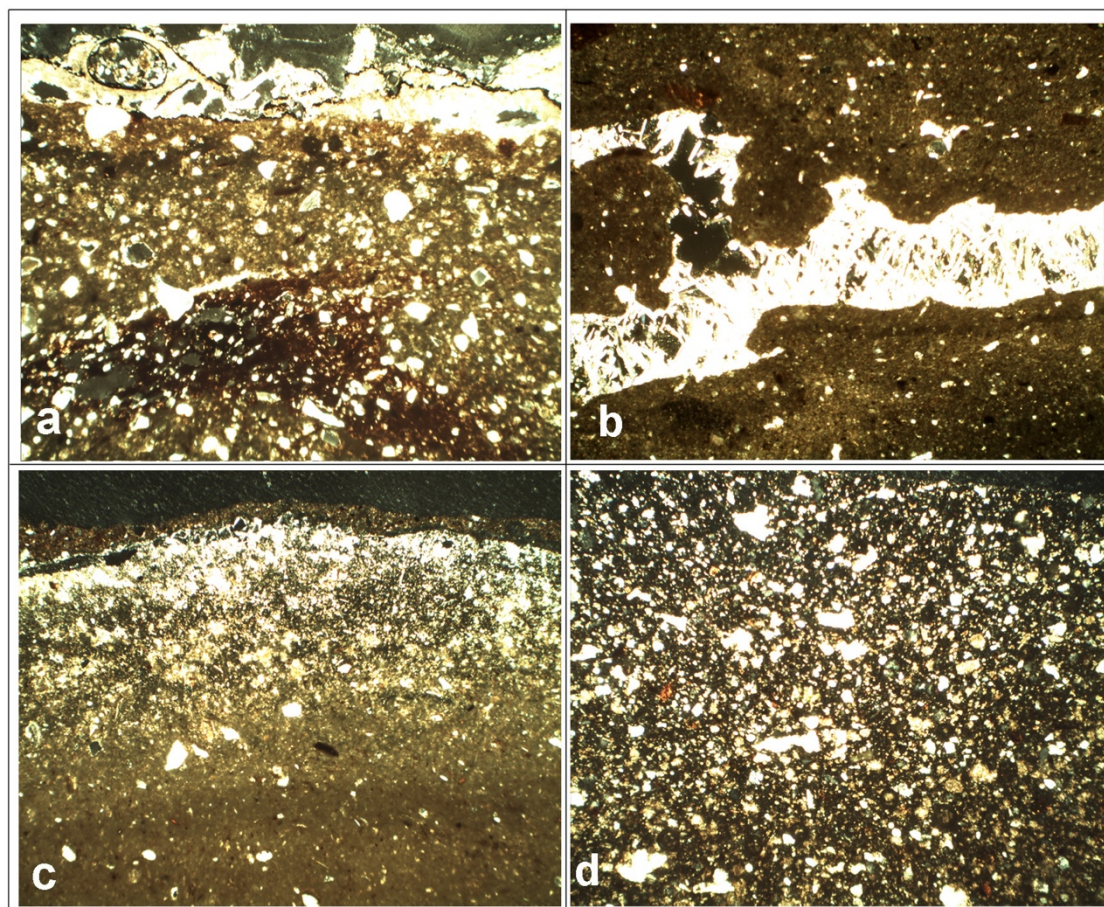


Figure 3. Thin section photomicrographs of the four main petrographic fabrics detected in amphorae sherds from terrestrial and underwater sites along the Dalmatian coast of the Adriatic, Croatia in this study. Fabric 1 (A); Fabric 2 (B); Fabric 3 (C); Fabric 4 (D). All images taken in crossed polars. Image width 2.9 mm

### Macroscopic and Microscopic Evidence for Alteration

Many of the analysed amphorae sherds contain macro- and microscopic evidence for alteration during burial. In hand specimen, samples from several shipwrecks exhibit bioencrustation (Quinn 2013: 206) on their exterior, left by the growth of marine invertebrate organisms with calcareous shells (Fig. 1B; 4A). This can be very thick and mask the shape of the original ceramic vessel. In thin section, both the precipitation and removal of carbonate material can be detected. Calcite can be seen infilling larger voids in samples of Fabric 1 from shipwrecks (Fig. 4B). This may have come from the re-distribution of carbonate material from the calcareous clay matrix and/or microfossil inclusions, or could have been allochthonous in origin (Cau Ontiveros *et al.* 2002). Secondary calcite is also present in voids in certain amphorae from terrestrial sites, e.g. Resnik/Siculi (Fig. 3A). Some sherds have distinct and often quite complex colour banding on a fresh break, for example amphorae from Vela Svitnja shipwreck in Fabric 1. This is caused in part by the dissolution of calcite from the sherd near its margins, which changes its colour relative to the core (Fig. 4C). Such banding is less prominent or not present at all in amphorae with thick bioencrustation, such as Fabric 3 sherds from the Žirje shipwreck. The bioencrustation may serve as a barrier, reducing the penetration of sea water into the fabric. Secondary calcite alteration is generally more intense in those amphorae samples recovered from the sea than on land (Fig. 4D). The core of the sherds in all four fabric groups remain unaltered and are thus most suited to the comparison of the petrographic and chemical

composition of samples from the two environments. The degree of alteration varies in its nature and severity between the four petrographic fabrics and between shipwreck sites.



*Figure 4. Thin section photomicrographs of post-depositional alteration within amphorae sherds from underwater and terrestrial sites along the Dalmatian coast of the Adriatic, Croatia in this study. Bioencrustation on the exterior of amphorae sherd (A). Secondary calcite deposited in voids in Fabric 1 (B); Layering in caused by the dissolution of calcite from the margins of Fabric 2 (C); Unaltered sherd of Fabric 1 recovered from land (D). All images taken in crossed polars. Image width 2.9 mm*

### **Geochemical Classification and Variability**

Multivariate statistical analysis of 33 elements was performed for each of the 168 amphora samples in order to reveal geochemical patterning and its correspondence with the petrographic fabrics classification (Appendix 1). Three samples (CG6, VS20 and SOK4) were removed from the dataset due to missing values for the elements As, Ni, Sr, respectively.

A plot of principal components 1 and 2 revealed a strong separation of the samples into three main groups, which correspond well with the petrographic fabric groups, with the exception of the association of the two Fabric 4 sherds with those of Fabric 2 (Fig. 5A). This pattern can be explained by low concentrations of Co, Fe and Ni in Fabric 1, high Co, Cr and Ni in Fabric 2, and high concentrations for a number of trace elements in Fabric 3 including Ce, Dy, Eu, Hf, La, Lu, Nd, Sb, Sm, Th, Ti, Yb and Zr (Fig. 5B). By labelling those amphorae that came from the shipwrecks versus those found on land (Fig. 5A), it is possible to see that these are not chemically identical within the same fabric group. This is particularly true for the samples

belonging to Fabric 1 (Fig. 5C) and the strong influence of Ca, Na, As, Ba, Sr and U on principal component 1 (Fig. 5D). It has been suggested that, due to contamination caused by burial environments and variability it introduces into composition of pottery, log-transformation can reduce these variables within a dataset (Buxeda I Garrigós 1999). Indeed, centred log ratio transformation has the effect of bringing together the marine and terrestrial samples in Fabric 1, which still overlap slightly (Fig. 5E). Assuming that amphorae within the same fabric groups have the same origin, hence the same geochemical composition, they should overlap in the PCA plot. However, the PCA with 32 elements in Fabric 1 shows that most of them are still chemically distinct from one another. (Fig. 5F).

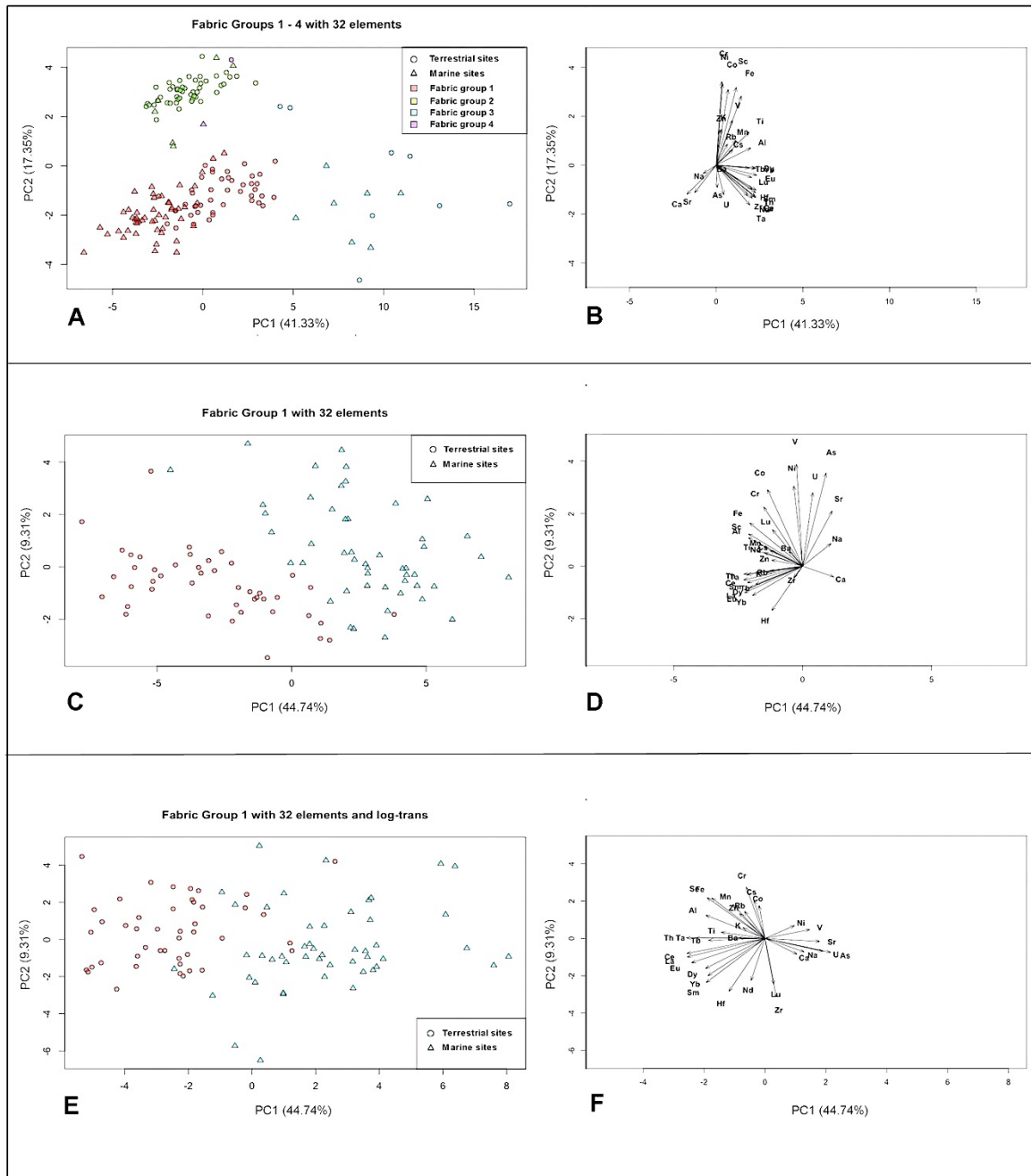


Figure 5. PCA scatterplots with 33 elements A) - PCA of non-transformed data in Fabric groups 1-4, B) - Loadings of the PCA of non-transformed data in Fabric groups 1-4, C) - PCA of non-transformed data in Fabric group 1, D) – Loadings of the PCA non-transformed data

*in Fabric group 1, E) -PCA with centred log- transformed data in Fabric group 1, F) – Loadings of the PCA with centred log- transformed data in Fabric group 1*

In order to examine in more detail elements that vary most within the four petrographic fabrics and differ consistently between those samples recovered from marine versus terrestrial environments, the coefficient of variation (CV) was calculated for Fabrics 1 – 3, but not for Fabric 4 since has only two samples (Table 2, Appendix 1). This revealed that the elements with a high CV, above 20%, in Fabrics 1 – 3 are Ca, Na, As, Ba, Cs, Ni, Rb, Sb, Sr and U. The three elements, K, Mn, Cr, and Zr have a CV > 20% in some fabrics, but are not consistent. For example, some elements, such as Mn and Zn have a CV > 20% in Fabric 1, Zn in Fabric 2 and Sb, Ta and Zr in Fabric 3. These variabilities may relate to different number of amphorae analysed from the marine and terrestrial environment in each fabric group, but also to mineralogical differences in the different amphorae fabrics. Also, the CV measures how much data is scattered around the central mean and, in our study, it did not give a clear answer as to how compositionally different are the marine and terrestrial amphorae in the same group of fabrics, nor which elements altered in the marine environment. Since the amphorae workshops in the region are still unknown, this prevents a direct comparison of the geochemical composition of Dalmatian amphorae recovered from shipwrecks with those from workshops. In that case, we could use a CV where the central mean would be known, but for our research, we applied test statistics.

Test statistics are based on testing hypotheses posed around research questions. It made it possible to investigate in detail whether there were significant differences between samples from the marine and terrestrial environment and to determine which elements were enriched or depleted in marine samples. In our study, we set up two hypotheses based on two research questions; do amphorae from the same fabric group, but buried in different environments, sea and land, have the same geochemical composition and if not, which elements cause this difference and are they enriched or depleted in samples from the marine environment? Because the test statistic compares two sample populations/groups, it can only be applied to compare groups with almost equal or equal sample size, or in our study, between the marine and terrestrial samples of Fabric 1 (n = 49/45) and Fabric 3 (n = 7/8) (Table 2). Unequal sample size in Fabric 2 with 6 marine and 50 terrestrial samples can significantly disturb the sample distribution in tests statistics.

Hypothesis tests begin with an F-test, which compares the two variances ( $\sigma^2$ ) and assesses whether the variances of the two populations, the group of samples from the marine environment (A) and the group of samples from the terrestrial environment (B), are equal. It determines whether two populations with a normal distribution have the same variance or, in simple words, whether the widths of the two distribution curves are equal. From this question, we set up a null hypothesis ( $H_0$ ) saying the variance of samples from marine environment, the group A ( $\sigma^2_A$ ) is equal to the variance of samples from terrestrial environment, the group B ( $\sigma^2_B$ ). An alternative hypothesis ( $H_1$ ) is that they are not equal. This can be explained as:

$$H_0: \sigma^2_A = \sigma^2_B$$
$$H_1: \sigma^2_A \neq \sigma^2_B$$

The calculated probability (p-value) of equal variances was determined by a significant alpha level of 0.05. If the p-value is equal to or greater than the alpha of 0.05, then the variance of group A is equal to the variance of group B and the null hypothesis can be accepted. On the other hand, if the p-value is lower than the alpha level, then variances of two groups are not equal and the null hypothesis is rejected or:

$$H_0 \text{ accepted: p-values} \geq \alpha$$

$$H_0 \text{ rejected: p-values} < \alpha$$

The results of F-tests for Fabric 1 (Table 2, Appendix 2) show that samples from the marine environment and samples from the terrestrial environment don't have equal variance for As, Ba, Hf, Mn, Na, Ni, Rb, Sm, Sr, U, Yb, Zn and Zr. In Fabric 3, unequal variance between the two samples groups are shown for As, Ce, Dy, Nd, U and Yb (Table 3, Appendix 2).

The second test statistic, with the t-test, compared the mean values and assessed the probability of changes in mean values between the two groups, samples from the marine and terrestrial environment. It allowed a detailed investigation of two possibilities, whether amphorae from the same group of fabrics, but from different environment, have the same geochemical composition, and if not, which elements cause compositional alterations and whether they have enriched or depleted in the marine environment. Similar to the previous F-test, the hypothesis was set; if there is not significant difference in the mean value between the samples from the marine and terrestrial environments, we can accept the null hypothesis and conclude that there were no alterations. Since we cannot estimate how the samples are distributed around the central mean, we applied the two-tailed Welch's test method using a standard alpha level of 0.05 (Fig. 6). Comparisons of the two mean values can be summarized:

$$H_0: \bar{x}_1 = \bar{x}_2$$

$$H_1: \bar{x}_1 \neq \bar{x}_2$$

Alternatively, if the mean values are different, then we can set up a new hypothesis based on whether the mean values of the elements in terrestrial samples are greater than the mean values in marine samples. If the p-values are equal to or greater than the alpha level of 0.05, then we can accept the null hypothesis and conclude that no, the mean value in the terrestrial samples is not greater than the mean value in the samples from the marine environment. Conversely, if the p-values are lower than the alpha 0.05 than the elements do have greater mean values and show a high possibility of alteration in the marine environment. This test was performed on one-tailed t-tests where the critical area of distribution is one-sided, which is either greater or less than the alpha value, but not both, as shown in Figure 6.

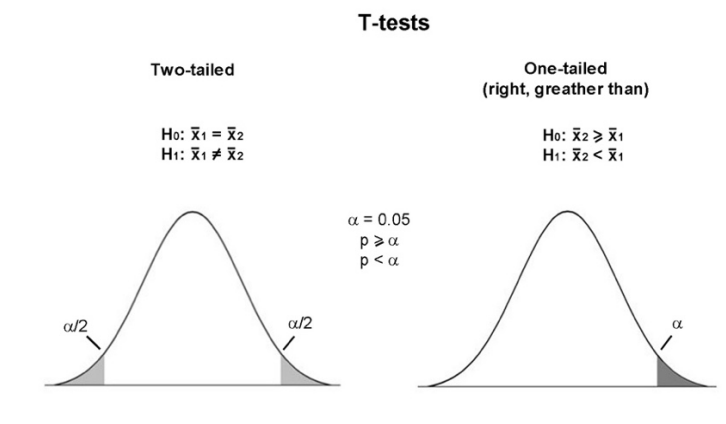


Figure 6: A) Illustration of two-tailed and one-tailed t-tests with significant alpha level of 0.05 and B) illustration of sample distribution with the same mean but unequal variances.

The t-test for Fabric 1 revealed that almost all elements, except Ca, Co, Ni and Zr, have significantly different mean values in samples from the marine and terrestrial environment (Table 2, Appendix 2). On the other hand, in Fabric 3 most elements did not show significant

changes in their mean values between samples from the marine and terrestrial environment, except for As, Ba, Cs, K, Na, Rb, Sb, and U (Table 2, Appendix 2). T-test for Fabric 1 showed that Al, Ca, Ce, Co, Cr, Cs, Dy, Eu, Fe, K, La, Lu, Nd, Sc, Ta, Tb, Th and Ti in the samples from terrestrial environment don't have greater mean values than the those from the marine environment. (Table 2, Appendix 2). In other words, although these 18 elements have different mean values in samples from the marine and terrestrial environment, the differences between them fall into a critical area of distribution and can be accepted as elements with less possibility of change.

Table 2: Summarise table for coefficient of variance (CV) of 33 elements in all samples in Fabric 1 and 3, with calculated mean values of the marine ( $\bar{x}_1$ ) and terrestrial ( $\bar{x}_2$ ) samples, p-values for F-test and t-tests (with e for standard scientific notation for powers of 10, e. g.  $p = 3.751e-10$  meaning, possibly value is  $3.751 \times 10^{-10}$ ). The mean, standard deviation and coefficient of variance of all samples in all examined fabric groups (Fabric 1 – 4) are presented in Appendix 1. The reports for F-test and t-tests are presented in Appendix 2.

Fabric 1							Fabric 3						
Element	All samples (n=94)	Marine (n = 49)	Terrestrial (n = 45)	F – test p-value > 0.05	T-test p-value > 0.05		Element	All samples (n=15)	Marine (n = 7)	Terrestrial (n = 8)	F – test p-value > 0.05	T-test p-value > 0.05	
	CV%	Mean ( $\bar{x}_1$ )	Mean ( $\bar{x}_2$ )	H <sub>0</sub>	H <sub>0</sub>	H <sub>1</sub>		CV%	Mean ( $\bar{x}_1$ )	Mean ( $\bar{x}_2$ )	H <sub>0</sub>	H <sub>0</sub>	H <sub>1</sub>
Al	14	61156	7094	0.46	3.751e-10	1	Al	8	77732	83712	0.26	0.1	0.95
As	67	26.1	10.5	3.626e-07	3.35e-11	/	As	74	42.2	13	0.0003	0.006	/
Ba	86	331.1	484.4	1.332e-15	0.02	/	Ba	33	229.1	395.2	0.83	0.0003	0.99
Ca	25	113407	106390	0.29	0.20	0.1	Ca	48	40213	36840	0.24	0.73	0.37
Ce	12	55.3	66.1	0.1	< 2.2e-16	1	Ce	13	88.1	97.5	0.04	0.14	0.92
Co	17	15.4	14.6	0.27	0.12	0.93	Co	15	24.2	24.1	0.21	0.96	0.48
Cr	21	108.2	126.7	0.91	0.0001	0.99	Cr	28	288.1	262.5	0.05	0.52	0.27
Cs	34	4.1	5.7	0.22	4.164e-06	1	Cs	48	4	9	0.97	0.0004	0.99
Dy	11	3.7	4.3	0.31	9.615e-13	1	Dy	14	5.4	5.8	0.02	0.25	0.86
Eu	11	1	1.2	0.09	< 2.2e-16	1	Eu	17	1.5	1.6	0.05	0.52	0.72

Fe	14	33675	39461	0.35	3.447e-09	1	Fe	10	46645	50106	0.37	0.17	0.90
Hf	18	4.2	3.7	0.009	0.0003	/	Hf	19	8.1	7.5	0.31	0.44	0.22
K	26	14596	18968	0.99	4.154e-06	1	K	29	12060	19316	0.98	0.0003	0.99
La	12	27.3	32	0.06	< 2.2e-16	1	La	15	44	46.3	0.05	0.5	0.73
Lu	13	0.3	0.3	0.06	0.02	0.98	Lu	12	0.4	0.4	0.67	0.98	0.49
Mn	25	728	954	0.02	5.357e-08	/	Mn	17	923.5	1086	0.85	0.07	0.96
Na	39	10394	6414	0.01	6.514e-11	/	Na	27	9058	6645	0.09	0.01	0.01
Nd	11	25	27	0.15	0.0005	0.99	Nd	17	38.2	38.5	0.01	0.91	0.53
Ni	35	60	52	0.02	0.06	0.03	Ni	38	160	157	0.06	0.93	0.47
Rb	42	70	106	0.0001	7.534e-07	/	Rb	38	64.2	123.7	0.75	0.0001	0.99
Sb	/	/	/	/	/	/	Sb	47	2.3	1.3	0.05	0.02	0.006
Sc	14	11.6	13.8	0.22	1.132e-11	1	Sc	15	15.2	16.7	0.09	0.21	0.88
Sm	11	5.1	6	0.0003	1.824e-13	/	Sm	15	7.8	7.9	0.08	0.79	0.59
Sr	37	538	388	1.069e-05	1.004e-05	/	Sr	44	163	147	0.77	0.67	0.33
Ta	14	0.9	1	0.62	1.048e-13	1	Ta	21	1.3	1.5	0.09	0.20	0.89
Tb	19	0.6	0.8	0.05	6.373e-14	1	Tb	17	1.1	1	0.38	0.64	0.32
Th	14	8.6	10.5	0.47	2.806e-16	1	Th	17	14.8	16.3	0.09	0.24	0.87

Ti	18	3088	3645	0.54	1.149e-06	1	Ti	9	4774	4710	0.33	0.77	0.38
U	43	3.5	2.6	2.831e-13	0.001	/	U	73	5.1	3.1	0.004	/	/
V	15	97	90	0.94	0.012	0.01	V	17	116	127	0.96	0.33	0.83
Yb	13	2	2.5	0.001	1.378e-12	/	Yb	14	3.2	3.4	0.03	0.39	0.79
Zn	29	92	120	0.0002	5.456e-06	/	Zn	15	109	118	0.08	0.31	0.83
Zr	18	107.1	107.8	0.002	0.86	0.54	Zr	23	224.4	200.1	0.68	0.36	0.18

Table 3: Summary of F-test and t-test for Fabric 1 with examples of boxplot for each result

	Equal variance	Unequal variance
<b>The same mean value</b>	<b>Ca, Co</b>	<b>Ni, Zr</b>
<b>Different mean values</b>	<b>Al, Ce, Cr, Cs, Dy, Eu, Fe, K, La, Lu, Nd, Sc, Ta, Tb, Th, Ti and V</b>	<b>As, Ba, Hf, Mn, Na, Rb, Sm, Sr, U, Yb and Zn</b>

To verify the results of test statistics, we conducted the PCA on 18 elements that, as mentioned above, show less possibility of alteration between the marine and terrestrial environment in Fabric 1. Although Ca showed no alteration in test statistics, based on previous PCA on Figure 5D, where it showed strong separation along its vector, we removed it from further analysis. The plot with remaining elements displays a good overlapping between samples from the marine and terrestrial environment (Fig. 7A). However, the loadings showed separation along Cs and K vectors (Fig. 7B). By removing those, the PCA on remaining 15 elements also showed good matching (Fig. 7C).

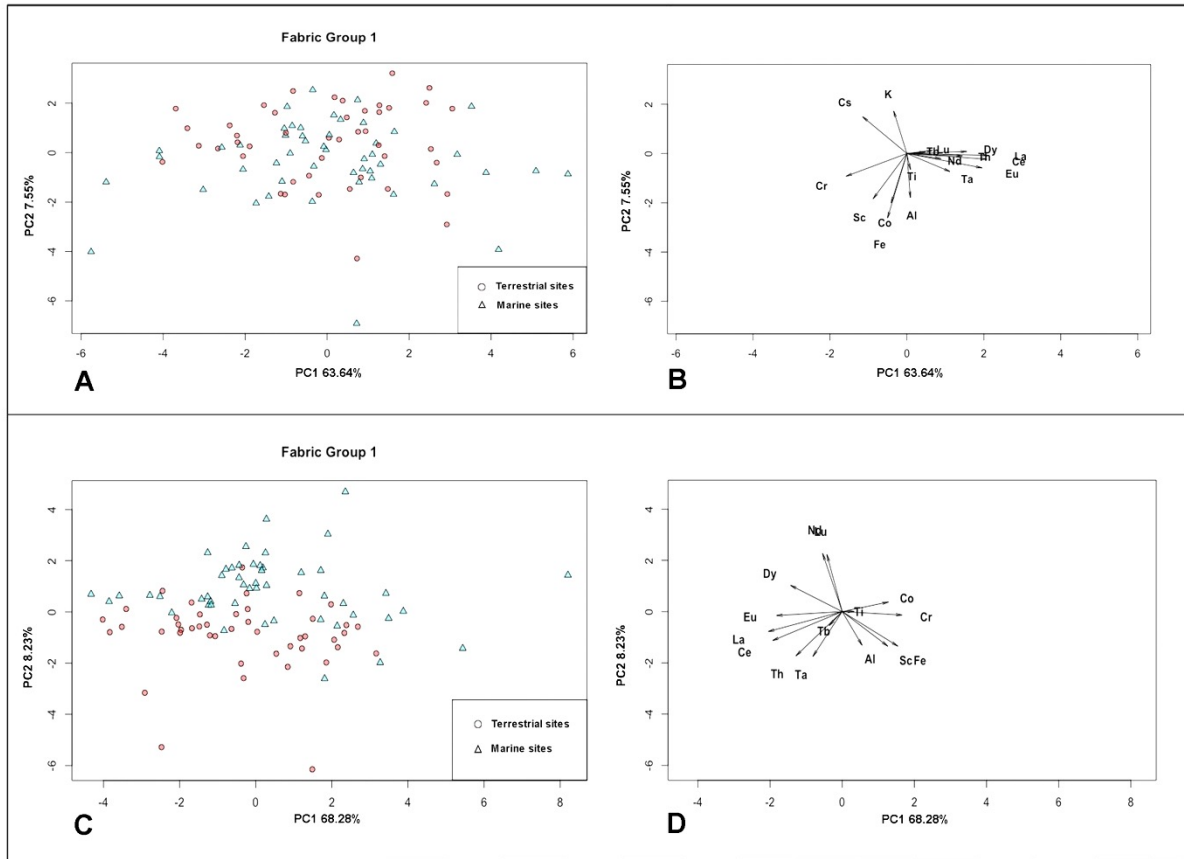


Figure 7. A) and B) - PCA plots of Fabric 1 with elements of less possibility of alterations, C) and D) – PCA plots of Fabric 1 with elements identified with test statistic of less possibility of alterations and excluded K and Cs. Both PCA were performed on centred log- transformed data

The results of test statistics for Fabric 1 and 3 showed that As and U in both groups have unequal variance, while Ba, Cs, K, Na and Rb have different mean values in samples from the marine and terrestrial environments. It also indicates that the concentration of these elements is likely to change in amphorae from the marine environment, regardless of the clay paste from which they are made. In addition, Ca concentration, as shown by PCA analysis, also has a high potential for change. Although Sr values in marine and terrestrial samples in Fabric 3 did not show a significant difference, the PCA plot in Figure 5B shows a strong separation. After removal of these elements and Sb, because it is not measured in some samples from the marine environment in the fabric 1, the PCA on four fabrics groups with remaining 23 elements (Al, Ce, Co, Cr, Dy, Eu, Fe, Hf, La, Lu, Mn, Nd, Sc, Sm, Ta, Tb, Th, Ti, V, Yb, Zn and Zr) confirmed that the marine and terrestrial samples overlap within each fabric (Fig. 8). It also showed a clear difference between the three groups, Fabric 1–3, while Fabric 4 again matched with Fabric 2. Separation between the Fabric 1 and 2 clusters along the Cr, Co, and Ni vectors suggests their regional differences.

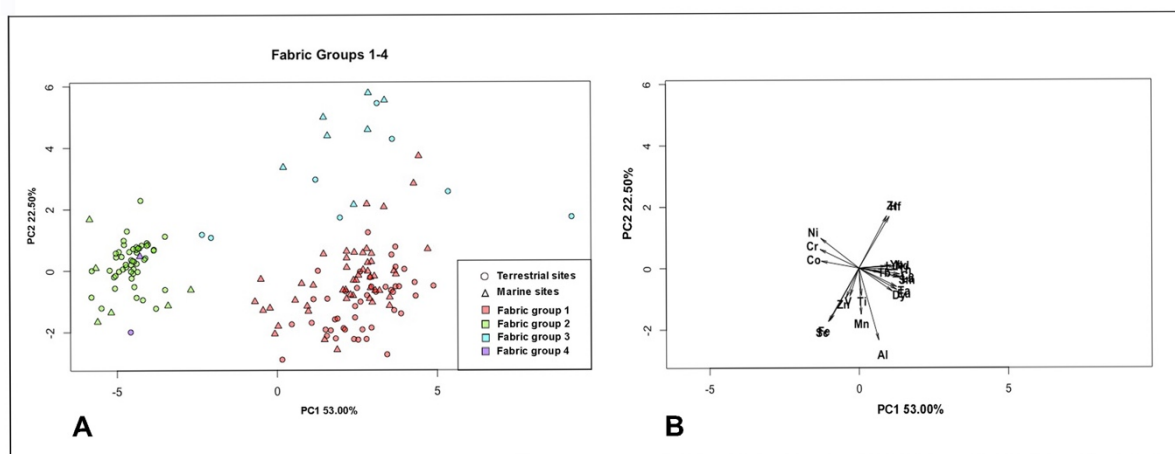


Figure 8. A) and B) - PCA plots of Fabric groups 1 – 4 on centered log- transformed data with elements identified with test statistic of less possibility of alteration.

Integrating the results of ceramic petrography with bulk geochemical analysis permitted a detailed examination on how different burial environments affect the geochemical composition of amphorae made of the same raw materials and technology. With test statistics and PCA, As, Ba, Ca, Cs, K, Na, Rb, Sb, Sr and U showed high possibility of alteration in all examined fabric groups. Among them, As, Ca, Na, Sb, Sr and U show an increase in the concentration in marine samples, which indicates enrichment, while the concentrations of Ba, Cs, K and Rb are reduced, which indicates leaching with seawater. In addition to these elements, the concentration of Ni and Cr also changed in Fabric 1. Although the CV of Cr is above 20%, it did not cause a significant shift in the whole data set, since these changes fall under the critical curve within t-test alternative hypothesis (Table 2). On the other hand, the CV of Ni is very high (35%), but its mean value in marine and terrestrial samples did not change significantly (Table 3). This situation is not uncommon, especially in very large groups of samples, as in the case of Fabric 1 (96 samples), when data may spread more within the population distribution. Besides, the variability in Cr and Ni concentrations may be related to the regional difference, so we kept them in the PCA analysis of four fabric groups. (Fig. 8).

## Discussion

Ceramic petrography and bulk geochemical analysis of a large number of Dalmatian Hellenistic and Roman Republican amphorae recovered from different burial environments, wrecks at the bottom of the sea and soil on land, has revealed microstructural and compositional alteration in amphorae from both environments. Long exposure to seawater can cause the formation of bioencrustation on the outer surfaces of amphorae (Fig. 4A). This organic encrustation does not form on all amphorae from shipwrecks and this may depend on the position of the amphorae at the site of the wreck and/or the seabed environment of the shipwreck. Namely, the amphorae from the Vela Svitnja shipwreck, laid in shallow waters on the northern side of the island of Vis (Fig. 4C), don't have bioencrustation, while amphorae from the shipwreck buried in deep waters near the island of Žirje (Fig. 4A) almost all have an organic encrustation on surface. Microstructural analyses of amphorae from different shipwrecks have shown that the bioencrustation on the outer surface prevents alteration. It serves as a barrier to prevent the inflow of seawater through the pores into the matrix of amphorae which can cause significant changes in their microstructure, such as dissolution of calcite and precipitation of secondary calcite.

Detailed analysis of amphorae by ceramic petrography revealed that dissolution of calcite is the main visible alteration in amphorae from the marine environment and is more concentrated on the margins. Parts of the amphorae matrix closer to both surfaces change colour relative to the core and it may cause sherds to have distinct and often quite complex colour banding on a fresh break, as shown in

the amphorae from Vela Svitnja shipwreck (Fig. 4C). The dissolution of calcite in pottery is not only caused by the marine environment, because it also takes place, as Maritan (2020) reports, within pottery from terrestrial environments.

Another microstructural alteration in amphorae is the precipitation of secondary calcite within voids in the clay matrix. This process can also occur in pottery buried in both environments, e. g. in amphorae from the port facilities in Resnik/Siculi (Fig. 3A) and in amphorae from the Vela Svitnja shipwreck (Fig. 4B). Precipitation of secondary calcite in amphorae from shipwreck has also been reported in previous studies (Buxeda I Garrigós *et al.* 2005; Martínez Ferreras *et al.* 2015), and in pottery buried in terrestrial sites (Freestone *et al.* 1985; Buxeda I Garrigós and Cau Ontiveros 1995; Buxeda I Garrigós 1999; Maritan and Mazzoli 2004; Belfiore *et al.* 2007; Maritan 2020). In our study, both processes were recognised in the calcareous matrix of Fabric 1, and this may have been due to the redistribution of carbonate material from the clay matrix and/or microfossil inclusions, as Cau Ontiveros *et al.* (2002) noted. Ceramic petrography has proved useful in detecting microstructural changes in pottery buried in the marine environment, but it has also shown that in the core of the samples there are no obvious alteration in fabric. It still allows direct comparison of fabrics and petrographic classification for provenance studies, as it is shown in our study of the Dalmatian amphorae.

Previous studies of amphorae from shipwrecks have identified the same elements with great potential for alteration in the marine environment (Nieto and Picon 1986; Taylor *et al.* 1997; Martínez Ferreras *et al.* 2015). The alkaline elements, such as Cs, K and Rb, are depleted in amphorae from the marine environment (Maritan 2020), as in our Fabrics 1 and 3. On the other hand, in the same fabrics, Sr is enriched in samples from the marine environments. This enrichment, according to Maritan (2020) may not be due to any secondary phase, as Sr may crystallise as carbonate, sulphate, borate, phosphate due to precipitation from aqueous solutions.

In addition to the 10 elements (As, Ba, Ca, Cs, K, Na, Rb, Sb, Sr and U), some trace elements in Fabric 1 also exhibit changes in their concentrations, especially by Ni enrichment and Cr depletion (Table 2). It has been suggested that differences in trace elements, such as Ni and Cr identified in the amphorae from the Port-Vendres 4 shipwreck off the coast of France, are the consequences of different amphorae origins within the cargo rather than seawater weathering processes (Martínez Ferreras *et al.* 2015). The difference in Cr and Ni concentration in Fabric 1 of Dalmatian amphorae, could be due to sample size, or consequence of the paste preparation process, as reported by Braekmans *et al.* (2011). The authors noted that during the levigation process of the raw material, most minerals are removed and the clay content drastically increases compositionally, such as Cr concentrations. However, more studies and experiments with raw material and different paste preparation recipes is needed to make full assessments of geochemical alterations in ceramic during production process (Miše *et al.* 2020). Besides, concentrations of Ba, Ca, Cs, K and Rb, may alter in pottery due to different terrestrial environments (Freestone 2001; Schwedt *et al.* 2004; Schneider 2016; Golitko *et al.* 2012). However, their enrichment or depletion depend on firing temperature, as well as their burial environment. This element, together with Cs, K and Rb, behaves differently in pottery buried in the marine and terrestrial environments. In Ca rich pottery from the marine environment, such as Fabric 1, and fired at high temperatures, they are depleted, but Ba and Cs are enriched in pottery buried in terrestrial environment fired at temperatures below 750°C (Freestone 2001; Mommsen 2001; Buxeda I Garrigós *et al.* 2002; Schneider 2016; Maritan 2020).

The same concentration of Ca in amphorae from the marine and terrestrial environment in Fabric 1 and 3 is the result of a sampling procedure for INAA analysis, where only the core of the sample is analysed. Removal of both surfaces and analysis of the sample core alone may provide less variability in data composition, as shown in our study and as suggested by Schneider (2016). A study by Schwedt *et al.* (2004) on pottery buried in soils also showed differences in Ca concentrations between samples

margin and core. Contrary to our research, where Ca increases near the surface in samples from the marine environment, the authors showed a decrease of Ca at the margins in samples from terrestrial environments and interpret this as part of the leaching process. It is clear that sea water affects the concentration of Ca differently, due to the highly distinctive process of dissolution of calcite in the amphorae from the marine environments, as shown by ceramic petrography (Fig. 4C). Although, there are no noticeable differences in Ca concentration in the samples core, other elements altered. The only explanation would be that As, Ba, Cs, K, Na, Rb, Sb, Sr and U altered in the core, whereas Ca did not.

The goal of studying the origins of amphorae from shipwrecks is the reconstruction of ancient maritime trade. However, post-depositional alterations in amphorae from the marine environment hamper their direct comparisons with amphorae from terrestrial sites, and thus finding their place of origin. By identify the processes that cause post-dispositional alteration in the amphorae buried in the marine environments, as well as understanding the effects of soils on the amphorae buried at terrestrial sites, we can mitigate this problem. The dissolution of calcite form at the margins of the samples, as shown by ceramic petrography, leaves the ceramic matrix in the core of the sample, in most cases, unchanged. Ceramic petrography has proved to be a useful method for studying pottery affected by post-depositional alterations in the marine environments, since the core of samples still provide sufficient information for fabric analysis. Accordingly, bulk geochemical analysis of the sample core reduces possibility of geochemical variability between amphorae from the marine and terrestrial environments. However, movable and alkaline elements, as well as As, Sb, Sr, and U, can be altered in both environments and in different fabrics. Test statistics have proven to be a useful tool for determining the enrichment and depletion of elements in marine samples, especially when reference groups from workshops are unknown and which can provide a direct comparison. Finally, some trace elements, such as Cr, Co and Ni, may show different behaviour in different fabrics and in different environments, and this could be caused by regional differences that are important for differentiating regional production and thus reconstructing the movement of amphorae.

## Conclusion

Petrographic and geochemical analyses of Hellenistic and Roman Republican transport amphorae recovered from shipwrecks and settlements along the maritime trade route in Dalmatia in southern Croatia, revealed four main petrographic and three geochemical groups. All fabric groups consist of amphorae recovered from the marine and terrestrial environments, which opened the possibility of investigating post-depositional alterations on pottery made by the same technological processes, paste preparations and firing temperatures, but which were exposed over two millennia to different environments, seawater and soils.

Ceramic petrography revealed microstructural changes in amphorae from the marine environment affected by the precipitation of calcite on margins of the sample and the formation of secondary calcite in voids. The latter process is also observed in samples from the terrestrial environment. The occurrence of both processes depends on the porosity of amphorae and the formation of bioencrustation on surface on amphorae from marine environments. Bioencrustation prevents the inflow of seawater into the clay matrix that causes the dissolution of calcite. This process is more pronounced at the margins of the sample, where the original ceramic fabric is not recognizable, while the ceramic matrix in the core of the sample, in most cases, remains unchanged and leaving enough information for petrographic analysis for provenance studies. Ceramic petrography has shown to be a useful method for studying pottery from different environments, as also previously noted by Buxeda I Garrigós *et al.* (2005). On the compositional level, the geochemical analysis of the sample core can reduce the variability of the data set introduced by post-depositional alterations. However, some elements have changed nonetheless. In our study, we identify the enrichment of As, Na, Sb, Sr and

U and depletion of Ba, Cs, K and Rb in amphorae from the marine environments in all studied fabric groups.

Identifying the process that causes post-dispositional changes in amphorae buried in the marine and terrestrial environment with ceramic petrography enables the establishment of a sampling strategy for geochemical analysis and statistical methodology. Sampling the core can reduce geochemical variability in the data set because, since it has been shown by ceramic petrography, changes that can cause enrichment of Ca are mainly occurring on the margins. On the other hand, some elements can alter in the core of the sample, such as As, Ba, Cs, K, Na, Rb, Sb, Sr and U. They are identified with test statistics, which proved to be a useful tool in identifying post-depositional alterations in amphorae from the marine environments, especially when reference groups from workshops are not available. Lastly, several steps should be implemented to mitigate the problem of comparing pottery buried in different environments and affected by different weathering processes; i) sampling the sample core for geochemical analysis, ii) applying, when possible, a statistical hypothesis testing when comparing groups of samples from different environments, and iii) complementing geochemical analysis with ceramic petrography. This could have a significant contribution to the studies of pottery provenances and can be implemented in the survey of maritime trade.

## Acknowledgements

The authors of the paper would like to thank Dr Branko Kirigin, Dr Sara Popović, Andrea Devlahović and Aldo Čavić from the City Museum in Stari Grad on Hvar, Boris Čargo from the Archaeological Museum in Split, Ivan Šuta from the Municipality Museum Kaštela, Dr Irena Radić Rossi and Dr Igor Borzić from the University of Zadar, Dr Domagoj Perkić from Dubrovnik Museums, Jurica Bezjak from the Croatian Conservation Institute, Department of underwater archaeology and Dr Vedran Barbarić from the University of Split for kindly providing the material for analysis. Many thanks to Dr Michael Charlton from the UCL Institute of Archaeology for his guidance and assistance with statistical analyses, and many colleagues for their suggestions and advice while researching this complex topic.

The research that have led to these results has received funding from the European Commission MSCA – IF, as part of the project *Economy of Pre-Roman Adriatic Communities: amphora production and trade patterns in a changing world*, EPRAC, Award Number: 177373 and a subsidy from US National Science Foundation grant number 191277.

## References

- Archibald, Z., H., 2013. Economy, Hellenistic, in: Bagnall, R. S, Brodersen, K., Champion, C. K. and Erskine, A., *The Encyclopedia of Ancient History*, First Edition: 2280–2285.
- Barone, G., Crupi, V., Galli, S., Longo, F., Majolino, D., Mazzoleni, P., and Spagnolo, G., 2004a. Archaeometric analyses on ‘Corinthian B’ transport amphorae found at Gela (Sicily, Italy), *Archaeometry*, 46: 553–568, <https://doi.org/10.1111/j.1475-4754.2004.00173.x>
- Barone, G., Crupi, V., Galli, S., Majolino, D., Migliardo, P., Spagnolo, G., 2004b. Mineralogical-petrographic and spectroscopic investigations on coarse potteries and transport amphorae from Agrigento. *Mediterranean Archaeometry and Archaeology* 4, 1, 47- 59.
- Barone, G., Lo Giudice, A., Mazzoleni, P., Pezzino, A., Barilando, D., Crupi, V. and Triscari, M., 2005. Chemical characterization and statistical multivariate analysis of ancient pottery from Messina, Catania, Lentini and Siracusa (Sicily). *Archaeometry* 47, 745- 762. <https://doi.org/10.1111/j.1475-4754.2005.00230.x>

- Barone, G., Crupi, V., Longo, F., Majolino, D., Mazzoleni, P., Spagnolo, G., Venuti, V., and Aquilia, E., 2011. Potentiality of non-destructive XRF analysis for the determination of Corinthian B amphorae provenance, *X-Ray Spectrometry*, 40: 333–337, <https://doi.org/10.1002/xrs.1347>.
- Barone, G., Mazzoleni, P., Aquilia, A., and Barbera, G., 2014. The Hellenistic and Roman Syracuse (Sicily) fine pottery production explored by chemical and petrographic analysis: *Archaeometry*, 56, 1: 70–87, <https://doi.org/10.1111/j.1475-4754.2012.00727.x>.
- Barra Bagnasco, M., Casoli, A., Chiari, G., Compagnoni, R., Davit, P., Mirti, P., 2001. Mineralogical and chemical composition of transport amphorae excavated at Locri Epizephiri (southern Italy). *Journal of Cultural Heritage* 2, 229 – 239.
- Belfiore, C. M., Day, P. M., Hein, A., Kilikoglou, V., La Rosa, V., Mazzoleni, P. and Pezzino, A., 2007. Petrographic and chemical characterization of pottery production of the Late Minoan I kiln at Haghia Triada, Crete, *Archaeometry*, 49, 4: 621–653. <https://doi.org/10.1111/j.1475-4754.2007.00324.x>
- Bevan, A., 2014. Mediterranean Containerization, *Current Anthropology*, 55.4: 387-418.
- Braekmans, D., Degryse, P., Poblome, J., Neyt, B., Vyncke, K., Waelkens, M., 2011. Understanding ceramic variability: an archaeometrical interpretations of the Classical and Hellenistic ceramics at Düzen Tepe and Sagalassos (Southwest Turkey). *Journal of Archaeological Science* 38, 9: 2011–2115. <https://doi.org/10.1016/j.jas.2011.02.003>
- Buxeda I Garrigós, J., 1999. Alteration and Contamination of Archaeological Ceramics: The Perturbation Problem, *Journal of Archaeological Science*, 26, 3: 295–313. <https://doi.org/10.1006/jasc.1998.0390>
- Buxeda I Garrigós, J. and Cau Ontiveros, 1995. Identificación y significado de la calcita secundaria en ceramias arqueológicas, *Complutum*, 6: 293-309.
- Buxeda I Garrigós, J., Mommsen, H., and Tsolakidou, A., 2002. Alterations of Na, K, and Rb concentrations in Mycenaean pottery and a proposed explanation using X-ray diffraction, *Archaeometry*, 44, 2: 187–198. <https://doi.org/10.1111/1475-4754.t01-1-00052>
- Buxeda I Garrigós, J., Cau Ontiveros, M. A., Madrid Fernandez, M. and Tonilo, A., 2005. Roman amphorae from Iulia Felix shipwrecks: alteration and provenance. In: Kars, H. and Burke, E. (Eds.), Proceedings of the 33<sup>rd</sup> International Symposium on Archaeometry, 22-26 April 2002, *Geoarchaeological and Bioarchaeological Studies* vol 3, Amsterdam: 149-151.
- Cambi, N., 1972. Vis, uvala Vela Svitnja - brodolom antičkog broda, *Arheološki pregled*, 14, Beograd: 80-82.
- Cambi, N., 1989. Anfore romane in Dalmazia. In: Amphores romaines et histoire économique. Dix ans de recherche. Actes du colloque de Sienna (22-24 mai 1986), *Publications de l'École française de Rome*, 114: 311-337.
- Carratoni, L., Iezzi, M and Meucci, C., 2016. Greco-Italic Amphorae from the Punta Romana Shipwreck (Sardinia – Italy), *Interdisciplinaria Archaeologica. Natural Sciences in Archaeology*, VII, 2: 179–187.
- Cau Ontiveros M. A., Day, P. M., Montana, G., 2002. Secondary calcite in archaeological ceramics: evaluation of alteration and contamination processes by thin section study. In: Kilikoglou V, Hein A, Maniatis, Y. (Eds) Proceedings of the 5th European meeting on ancient ceramics modern trends in scientific studies on ancient ceramics, *BAR International Series* 1011, Oxford: 9–18.
- Ceccarelli, L., Rossetti, I., Primavesi, L. and Stoddart, S., 2016. Non-destructive method for the identification of ceramic production by portable X-rays Fluorescence (pXRF). A case study of

- amphorae manufactures in central Italy. *Journal of Archaeological Science: Reports*, 10: 253–262. <http://dx.doi.org/10.1016/j.jasrep.2016.10.002>
- Day, P. M., Quinn, P. S., Kilikoglou, V. and Rutter, J. A. 2011. A World of Goods: Transport Jars and Commodity Exchange at the Late Bronze Age Harbor of Kommos, Crete. *Hesperia*, 80: 511-558.
- Fantuzzi, L., Cau Ontiveros, M. A. and Aquilué, X., 2016. Archaeometric Characterization of Amphorae from the Late Antique City of Emporiae (Catalonia, Spain), *Archaeometry*, 58, 51: <https://doi.org/10.1111/arcm.12176>
- Fantuzzi, L., Cau Ontiveros, M. A., Macias Sole, J. M. and Martorell, R., 2019. Eastern Mediterranean Amphorae from Late Antique Urban Centers of the Northeastern Iberian Peninsula: Archaeometric Characterisation. *ArchaeoSciences*, 43, 2: 229–247. <https://doi.org/10.4000/archeosciences.6897>
- Farnsworth, M., Perlman, I., and Asaro, F., 1977. Corinth and Corfu: A Neutron Activation Studies of their Pottery, *American Journal of Archaeology*, 81, 4: 455-468.
- Finocchiaro, C., Barone, B., Mazzoleni, P. and Spagnolo, G., 2018. New insights on the Archaic ‘Corinthian B’ amphorae from Gela (Sicily): The contribution of the analyses of Corfu raw materials, *Mediterranean Archaeology and Archaeometry*, 18, 5: 179-189. DOI: 10.5281/zenodo.1285908
- Freestone, I. C., 2001. Post-depositional changes in archaeological ceramics and glasses. In: Brothwell, D. R. and Pollard, A., M. (Eds), *Handbook of Archaeological Science*, John Wiley, New York: 615-625.
- Freestone, I. C., Meeks, N. D., and Middleton, A. P., 1985. Retention of phosphate in buried ceramics: an electron microbeam approach, *Archaeometry*, 27, 2: 161–77. <https://doi.org/10.1111/j.1475-4754.1985.tb00359.x>
- Gibbins, D., 2001. Shipwrecks and Hellenistic trade. In: Archibald, Z. H., Davies, J. K., Gabrielsen, V., and Oliver, G. J., (Eds.), *Hellenistic economies*, London: 273-312.
- Gluscock, M. D., 1992. Characterization of Archaeological Ceramics at MURR by Neutron Activation Analysis and Multivariate Statistics. In: Neff, H., (Ed.), *Chemical Characterization of Ceramic Paste in Archaeology*, Prehistory Press, Madison: 11-26.
- Golitko, M., Dudgeon J. V., Neff, H. and Terrell J. E., 2012. Identification of Post-Depositional Chemical Alteration of Ceramics from the North Coast of Papua New Guinea (Sanduan province) by Time-of-Flight–Laser Ablation–Inductively Coupled Plasma–Mass Spectrometry (TOF–LA–ICP–MS), *Archaeometry* 54, 1: 80-100. <https://doi.org/10.1111/j.1475-4754.2011.00612.x>
- Hein, A., 2014. Revisiting the Groups – Exploring the Feasibility of Portable EDXRF in Provenance Studies of Transport Amphorae in the Eastern Aegean, in: Hegewisch, M., Daszkiewicz, M. and Schneider, G. (Eds.), *Using pXRF for the Analysis of Ancient Pottery – an Expert Workshop in Berlin 2014*, *Berlin Studies of the Ancient World* 75: 41-58. DOI: 10.17171/3-75
- Hein, A., Georgopoulou, V., Nodarou, E. and Kilikoglou, V., 2008. Koan amphorae from Halasarna – investigation in a Hellenistic amphora production centre, *Journal of Archaeological Science* 35, 4: 1049-1061. <https://doi.org/10.1016/j.jas.2007.07.009>
- Horden, P. and Purcell, N., 2000. *The Corrupting Sea. A Study of Mediterranean History*, Oxford.
- Koehler, C. G., 1979. *Corinthian A and B transport amphoras*, Princeton University Press, Princeton.
- Koehler, C. G., 1981. Corinthian developments in the study of trade in the fifth century, *Hesperia*, 50, 4: 449-458.
- Machut, P., Ben Amara, A., Cantin, N., Chapoulie, R., Frèrebeau, N., F.-X. Le Bourdonnec, Marion, Y. and Tassaux, F., 2015. Towards high resolution ceramic series for production site studies: the case

- of Loron amphorae (Croatia, 1st–3rd c. A.D.), *Heritage Science*, 21, 3. <https://doi.org/10.1186/s40494-015-0050-5>
- Maritan, L., 2020. Ceramic abandonment. How to recognise post-depositional transformations, *Archaeological and Anthropological Sciences*, 12:199 <https://doi.org/10.1007/s12520-020-01141-y>
- Maritan, L., and Mazzoli, C., 2004. Phosphates in archaeological finds: implications for environmental conditions of burial, *Archaeometry*, 46, 4: 673–683. <https://doi.org/10.1111/j.1475-4754.2004.00182.x>
- Maritan, L. Mazzoli, C., Mazzocchin, S. and Cipriano, S. 2019. Provenance of wine and oil amphorae from the Northern Adriatic: archaeometric and epigraphic Approaches. *ArchaeoSciences*, 43, 2: 203–210. <https://doi.org/10.4000/archeosciences.6732>
- Martínez Ferreras, V., Buxeda I Garrigós, J., Gurt I Esparraguera, J. M. and Kilikoglou, V., 2007. Archaeometric characterisation of roman wine amphorae from Barcelona (Spain), in: Waksman, S. Y. (ed.), *Archaeometric and Archaeological Approaches to Ceramics. Papers presented at EMAC '05, 8th European Meeting on Ancient Ceramics, Lyon 2005, BAR International Series 169*: 113–119.
- Martínez Ferreras, V., Capell, C., Jézégou, M.-P., Salvat, M., Castellvi, G. and Cabella, R., 2015. The Port-Vendres 4 shipwreck cargo: evidence of the Roman wine trade in the Western Mediterranean, *Journal of Nautical Archaeology*, 44, 2: 277–299. <https://doi.org/10.1111/1095-9270.12109>
- Miriello, D., Bloise, A., De Luca, R., Apollaro, C., Crisci, G. M., Medaglia, S. and Taliano Grasso, A., 2015. First compositional evidences on the local production of Dressel 2–4 amphorae in Calabria (Southern Italy): characterization and mixing simulations, *Appl. Phys. A*, 119: 1595–1608. <https://doi.org/10.1007/s00339-015-9143-y>
- Miše, M., Serneels, V., Matana, A., Montanari, A., and Kirigin B., 2019. Provenience studies of amphorae from the Greek colony Pharos on the island of Hvar, Croatia. In: Koeberl, C., Bice, D. M., (Eds), 250 Million Years of Earth History in Central Italy: Celebrating 25 Years of the Geological Observatory of Coldigioco, *Geological Science of America. Special Papers*: 542: 471–499. [https://doi.org/10.1130/2019.2542\(27\)](https://doi.org/10.1130/2019.2542(27))
- Miše, M., Quinn, P., Charlton, M., Serneels, V. and Montanari, A., 2020. Production and circulation of Late Hellenistic fine table ware in Central Dalmatia, Croatia, *Journal of Archaeological Science: Reports* 33 <https://doi.org/10.1016/j.jasrep.2020.102537>
- Mommsen, H., 2001. Provenance determination of pottery by trace element analysis: Problems, solutions and applications. *Journal of Radioanalytical and Nuclear Chemistry* 247: 657–662. <https://doi.org/10.1023/A:1010675720262>
- Montana, G., Randazzo, L., Belfiore, C. M., La Russa, M. F., Ruffolo, S. A., De Francesco, A. M., Antonino Pezzino, Punturo, R., and Di Stefano, V., 2014. An original experimental approach to study the alteration and/or contamination of archaeological ceramics originated by seawater burial, *Periodico di Mineralogia*, 83, 1: 89–120. <https://doi.org/10.2451/2014PM0006>
- Moreno Megías, V., García Fernández, F. J., Fragnoli, P. and Sterba, J. H., 2020. Petrographic and neutron activation analysis of Late Iron Age amphorae from the south western Iberian Peninsula, *Journal of Archaeological Science: Reports*, 34, <https://doi.org/10.1016/j.jasrep.2020.102598>.
- Nieto, J. and Picon, M., 1986. El pecio Culip IV : observaciones sobre la organización de los talleres de Terra sigillata de La Graufesenque, *Archaeonautica*, 6: 81–119. <https://doi.org/10.3406/nauti.1986.891>
- Olcese, G. 2007: The production and circulation of Greco-Italic amphorae of Campania (Ischia/Bay of Naples). The data of the archaeological and archaeometric research. *SKYIIS*, 60–75.

- Papadopoulos, J. K. and Paspalas, S., 1999. Mendaian as Chalkidian Wine, *Hesperia* 68, 2: 161-188.
- Parker, A. J., 1992. Ancient Shipwrecks of the Mediterranean and the Roman Provinces, *BAR Inter. Ser.* 580: Oxford.
- Peacock, D. P. S., 1977. Roman amphorae: typology, fabric and origins. In: Méthodes classiques et méthodes formelles dans l'étude typologique des amphores. Actes du colloque de Rome, 27-29 mai 1974., *Publications de l'École française de Rome*, 32: 261-278.
- Pecchioni, E., Cantisani, E., Pallecchi, P., Fratini, F., Buccianti, A., Pandeli, E., Rescic, S. and Conticelli, S., 2007. Characterization of the amphorae, stone ballast and stowage materials of the ships from the archaeological site of Pisa–San Rossore, Italy: Inferences on their provenance and possible trading routes, *Archaeometry*, 49, 1: 1–22. <https://doi.org/10.1111/j.1475-4754.2007.00285.x>
- Picon, M. and Empereur, J.-Y., 1986. Des ateliers d'amphores à Paros et à Naxos, *Bulletin de correspondance hellénique*, 110, 1: 495-511. <https://doi.org/10.3406/bch.1986.1811>
- Pradell, T., Vendrell, M., Krumbein, W. E. and Picon, M., 1996. Altérations de céramiques en milieu marin : les amphores de l'épave romaine de la Madrague de Giens (Var), *Revue d'Archéométrie*, 20 : 47-56. <https://doi.org/10.3406/arsci.1996.936>
- Quinn, S. P., 2013. *Ceramic Petrography. The Interpretation of Archaeological Pottery & Related Artefacts in Thin Section*, Oxford: Archaeopress.
- Schneider, G., 2016. Mineralogical and Chemical Alteration. In: Hunt, A. (Ed), *The Oxford Handbook of Archaeological Ceramic Analysis*, Oxford University Press. DOI: 10.1093/oxfordhb/9780199681532.013.11
- Schwedt, A., Mommsen, H., and Zacharias, N., 2004. Post-depositional elemental alterations in pottery: neutron activation analyses of surface and core samples, *Archaeometry*, 46, 1: 85–101. <https://doi.org/10.1111/j.1475-4754.2004.00145.x>
- Secco, M., Maritan, L., Mazzoli, C., Lampronti, G., Zorzi, I. F., Nodari, L., Russo, U. and Mattioli, S. P., 2011. Alteration processes of pottery in lagoon-like environments, *Archaeometry*, 53, 4: 809–829. <https://doi.org/10.1111/j.1475-4754.2010.00571.x>
- Swift, K., 2011. Archaic to Late-Republican transport amphorae. In. Carter, J., and Pietro, A., (Eds.), *The Chora of Metaponto 3. Archaeological Field Survey, Bradano to Basento*, Volume 1: Austin, Texas: 455–488.
- Taylor, R. J., Gibbins, D. J. L. and Robinson, V. J., 1997. An investigation of the provenance of the Roman amphorae cargo from the Plemmirio B shipwreck, *Archaeometry*, 39, 1: 9-21. <https://doi.org/10.1111/j.1475-4754.1997.tb00787.x>
- Tzochev, Ch., 2009. Notes on the Thasian amphorae stamps chronology, *Archaeologia Bulgarica* XIII, 1: 55-72.
- Whitbread, I. K., 1995. Greek Transport Amphorae. A Petrological and Archaeological Study: *The British School at Athens, Fitch Laboratory Occasional Paper* 4. Athens.

**Appendix 1:** Geochemical compositions of Fabric groups 1 – 4 (Tables 1 – 4), with mean, standard deviation (SD) and coefficient of variance (CV in %) for each fabric group

*Table 1A: Geochemical composition of analysed amphorae from Group 1 measured by INAA*

Sample	Site	As	La	Lu	Nd	Sm	U	Yb	Ce	Co	Cr	Cs	Eu	Fe	Hf	Ni	Rb	Sb
SGP1	Land	10.6	31.9	0.4	27.4	5.8	2.6	2.5	64.4	18.9	133.8	10.2	1.2	37686.9	4.2	99.4	106.1	1.8
SGP18	Land	40.5	34.2	0.4	28.5	6.0	4.3	2.7	68.5	19.0	164.1	8.2	1.3	48393.7	3.8	84.8	132.4	1.2
SGP23	Land	12.3	27.0	0.3	22.0	5.0	3.0	2.0	52.5	12.1	89.7	3.9	1.0	30342.8	3.5	56.7	83.5	0.5
SGP27	Land	13.4	31.2	0.4	26.5	5.8	2.7	2.3	63.6	13.2	95.2	5.1	1.1	35345.5	4.3	43.8	105.5	0.7
RES1	Land	11.4	33.4	0.3	25.8	6.0	2.6	2.3	64.9	12.7	133.2	6.6	1.2	40112.2	4.0	26.7	75.8	0.7
RES2	Land	9.9	33.3	0.4	28.4	6.1	2.3	2.5	66.7	16.5	132.9	4.9	1.2	41955.7	4.1	40.6	93.1	0.8
RES3	Land	15.9	33.8	0.4	27.5	6.2	2.4	2.2	67.3	14.3	101.3	5.3	1.2	36157.4	4.6	46.0	98.3	0.6
RES4	Land	10.2	32.8	0.4	30.9	5.9	2.4	2.6	64.9	13.7	106.1	2.8	1.2	39886.1	3.9	55.8	59.1	0.7
RES10	Land	17.0	34.6	0.4	25.9	6.2	2.7	2.6	69.8	18.6	117.6	4.6	1.3	43272.0	4.2	56.5	85.7	0.7
RES12	Land	13.2	32.7	0.3	27.9	5.8	2.4	2.4	66.8	17.8	140.6	6.0	1.2	42439.9	4.1	47.2	107.6	0.6
RES13	Land	12.7	34.6	0.4	26.6	6.3	3.1	2.8	71.2	16.9	156.6	7.0	1.2	37436.2	5.7	80.1	104.8	0.8
RES14	Land	6.7	32.5	0.4	24.8	5.9	2.8	2.4	66.0	17.5	172.3	6.2	1.2	41827.0	4.3	50.2	109.4	0.6
RES15	Land	10.9	33.3	0.4	26.6	6.0	1.9	2.6	69.6	17.8	89.6	4.0	1.2	39689.4	4.6	55.2	82.3	0.6
RES17	Land	12.0	28.8	0.3	25.3	5.3	2.5	2.6	58.5	10.4	125.3	5.8	1.1	34311.5	3.8	29.5	60.8	0.7
RES19	Land	11.1	31.3	0.4	28.0	5.6	2.4	2.6	61.1	14.9	118.1	2.2	1.2	36725.7	3.8	61.6	59.3	0.6
RES20	Land	6.4	34.9	0.4	29.5	6.3	3.0	2.7	70.5	18.4	160.4	4.0	1.3	46563.7	4.3	58.9	83.3	0.5
RES22	Land	16.8	35.1	0.4	30.4	6.4	2.4	3.0	70.3	16.5	126.0	5.1	1.3	40856.6	4.8	48.7	101.9	0.7
RES23	Land	13.1	35.8	0.4	29.4	6.5	2.7	3.0	70.3	15.3	122.2	5.3	1.3	40353.5	5.0	55.8	101.6	0.8
RES24	Land	11.9	31.9	0.3	25.8	5.7	2.3	2.5	63.8	13.5	109.0	6.1	1.1	37081.7	4.5	32.8	107.2	0.5
RES25	Land	13.5	37.6	0.4	29.6	6.5	3.4	2.7	75.1	18.9	159.5	7.1	1.3	46700.4	4.2	53.6	128.4	0.7
RES27	Land	10.9	34.0	0.4	29.2	6.1	2.8	2.7	70.7	16.8	164.3	3.7	1.2	45070.4	4.7	69.3	91.8	0.7
RES28	Land	11.3	29.9	0.3	25.1	5.4	2.7	2.4	57.1	13.3	125.8	3.8	1.1	38023.5	3.4	62.8	53.5	0.6
RES30	Land	12.1	34.8	0.4	27.5	6.4	2.8	2.9	71.6	17.4	143.5	4.1	1.3	45039.9	4.5	44.8	90.3	0.9
RES32	Land	6.3	34.9	0.4	29.9	6.1	2.6	2.6	69.7	18.0	149.3	5.0	1.3	45148.6	3.8	55.2	84.3	0.6
RES33	Land	10.4	30.0	0.3	26.6	5.4	2.8	2.4	59.7	14.5	93.8	4.2	1.1	36386.4	3.4	50.9	65.9	0.7

RES35	Land	8.1	36.5	0.4	31.1	6.7	2.2	2.6	74.5	14.8	100.5	5.7	1.4	39294.1	4.5	63.7	115.9	0.7
RAT1	Land	5.5	34.6	0.3	26.7	5.9	2.9	2.4	70.2	12.9	98.1	5.7	1.2	35801.0	4.4	75.3	75.3	0.6
SOK6	Land	8.4	29.6	0.3	24.9	5.4	2.1	2.3	57.3	12.8	113.9	4.3	1.1	34568.2	3.5	48.9	78.1	0.4
VS1	Shipwreck	12.7	26.0	0.3	23.7	4.9	2.3	2.0	51.8	11.9	104.3	5.0	1.0	30276.4	3.3	32.7	38.9	0.0
VS3	Shipwreck	16.2	26.8	0.3	23.7	5.1	4.7	1.8	54.5	12.5	97.1	4.4	0.9	30259.6	3.7	30.4	87.2	0.0
VS4	Shipwreck	33.6	26.0	0.3	21.6	4.9	2.3	2.3	51.0	13.3	99.4	2.4	1.0	32518.6	3.6	55.4	67.3	0.0
VS5	Shipwreck	13.2	26.3	0.3	24.4	5.0	2.8	1.9	51.8	13.4	102.7	1.1	1.0	29642.8	3.5	57.8	40.7	0.0
VS6	Shipwreck	26.8	24.7	0.3	22.1	4.8	4.0	1.8	48.5	11.4	105.0	3.7	0.9	28982.8	3.1	60.8	75.3	0.0
VS7	Shipwreck	17.6	26.6	0.3	24.0	5.1	2.7	2.2	52.9	13.7	107.6	4.8	1.0	32242.7	3.4	26.8	45.8	0.0
VS9	Shipwreck	11.1	24.9	0.3	22.2	4.8	2.3	1.9	51.0	14.5	96.1	3.4	1.0	29479.5	3.6	37.2	82.6	0.0
VS10	Shipwreck	34.0	29.0	0.3	24.5	5.4	3.3	1.9	58.5	14.1	104.2	4.4	1.0	31927.4	4.3	44.7	87.6	0.0
VS11	Shipwreck	16.0	26.8	0.3	24.4	5.1	2.7	2.1	52.0	14.6	106.9	5.1	1.0	32003.6	3.5	45.1	51.2	0.0
VS13	Shipwreck	15.0	29.6	0.3	24.5	5.4	2.5	2.1	57.1	14.0	97.9	2.4	1.1	33980.1	3.9	49.6	66.8	0.0
VS14	Shipwreck	28.5	28.2	0.3	24.7	5.4	4.1	2.1	56.6	14.3	102.4	3.4	1.0	33543.8	3.6	43.5	66.9	0.0
VS15	Shipwreck	14.5	27.4	0.4	24.6	5.2	4.2	2.3	54.7	12.4	115.4	2.4	1.0	30780.0	3.6	26.4	50.0	0.0
VS16	Shipwreck	46.4	25.6	0.4	23.3	5.2	8.7	1.8	51.3	14.0	98.0	4.3	0.9	28474.8	3.2	57.7	87.7	0.0
VS17	Shipwreck	18.2	28.1	0.3	27.0	5.2	2.4	2.0	53.9	12.9	108.8	4.5	1.0	32616.3	3.4	64.6	60.7	0.5
VS18	Shipwreck	17.9	27.3	0.3	24.2	5.1	2.4	2.1	53.5	11.7	102.5	3.7	1.0	31599.9	3.7	32.9	78.5	0.0
VS19	Shipwreck	28.4	28.3	0.3	25.4	5.3	3.0	2.0	56.5	13.0	105.1	4.7	1.0	30759.6	4.1	35.2	93.6	0.0
VS20	Shipwreck	14.5	24.4	0.3	20.7	4.5	2.3	1.9	47.4	12.6	95.8	4.5	0.9	30060.1	2.6	0.0	81.2	0.0
VS21	Shipwreck	44.5	28.5	0.3	25.0	5.4	3.1	2.1	55.7	18.3	118.8	5.3	1.1	37045.9	3.6	75.5	50.2	0.0
VS22	Shipwreck	32.9	31.2	0.3	28.7	5.8	2.7	2.2	61.6	21.3	126.8	5.3	1.2	43126.7	4.0	76.3	60.7	0.0
VS24	Shipwreck	12.2	30.1	0.3	24.8	5.5	2.0	2.3	59.6	14.2	93.3	5.3	1.1	28525.6	4.3	47.9	51.5	0.0
VS25	Shipwreck	14.3	26.2	0.3	23.3	5.1	3.3	2.0	52.1	12.9	113.6	5.5	1.0	30120.0	3.4	49.1	43.1	0.0
VS26	Shipwreck	22.0	26.8	0.3	23.9	4.9	2.4	2.2	52.9	12.2	87.8	4.1	1.0	31476.2	3.3	51.2	80.3	0.0
VS27	Shipwreck	31.7	25.2	0.3	24.1	4.8	2.3	2.0	49.2	17.0	99.9	2.6	0.9	31289.1	3.4	60.6	67.1	0.0
VS28	Shipwreck	16.3	25.9	0.3	23.0	4.8	2.3	2.0	51.1	12.0	69.0	2.3	0.9	27674.2	3.2	34.3	55.4	0.0
VS29	Shipwreck	28.4	28.4	0.4	25.2	5.6	9.1	2.2	57.7	14.1	112.5	3.4	1.0	35033.6	3.2	46.1	76.9	0.0
VS30	Shipwreck	22.1	29.3	0.3	26.9	5.4	3.2	2.4	57.8	12.9	94.5	5.6	1.1	35798.8	3.8	65.6	106.9	0.0
VS31	Shipwreck	12.4	23.7	0.3	23.4	4.5	2.5	2.0	45.6	10.4	99.8	4.9	0.9	27326.1	3.0	34.7	31.3	0.0
VS32	Shipwreck	23.2	23.9	0.3	23.6	4.5	2.1	1.7	47.3	13.3	80.3	1.8	0.9	29445.2	3.2	57.6	50.0	0.0
POL1	Shipwreck	39.5	30.1	0.4	26.6	5.5	2.9	2.4	63.3	14.3	118.3	6.5	1.1	38070.0	3.7	72.5	108.1	0.9
POL3	Shipwreck	36.0	26.8	0.5	25.6	5.3	4.7	2.2	56.5	19.0	145.3	3.0	1.1	44484.4	4.5	72.0	76.3	1.1

POL4	Shipwreck	21.8	29.4	0.3	26.9	5.3	3.2	2.1	59.5	15.9	121.0	5.2	1.1	36901.7	3.5	67.7	92.3	0.7
POL5	Shipwreck	24.3	28.0	0.3	21.7	5.0	2.6	2.0	59.2	15.9	120.2	4.5	1.0	38589.7	3.2	66.3	90.0	0.6
POL7	Shipwreck	23.7	25.1	0.3	25.5	4.7	2.9	1.9	51.5	12.2	96.8	3.9	1.0	30047.0	3.6	51.4	35.6	0.4
POL8	Shipwreck	8.8	29.1	0.3	25.2	5.2	2.4	2.1	60.0	15.7	122.8	5.7	1.0	38099.2	3.4	52.9	110.0	0.4
POL9	Shipwreck	19.3	31.5	0.3	30.4	5.7	2.4	2.3	65.3	21.7	206.5	6.8	1.1	45745.0	3.4	136.6	115.4	1.2
POL11	Shipwreck	42.1	23.9	0.3	32.8	4.5	2.7	1.9	48.9	12.6	154.1	2.9	1.0	30713.2	3.4	55.7	31.7	0.6
POL14	Shipwreck	37.8	28.9	0.3	27.7	5.3	3.8	2.1	59.8	13.8	113.9	5.5	1.1	36564.5	3.7	61.8	91.9	0.9
POL17	Shipwreck	20.5	28.2	0.4	24.4	5.3	3.7	2.3	57.7	14.5	100.4	3.2	1.0	31006.9	4.3	104.6	72.3	0.8
POL18	Shipwreck	73.7	28.1	0.4	25.9	5.2	5.9	2.0	58.0	16.1	120.1	4.1	1.0	37680.8	3.1	77.5	99.9	0.8
POL19-1	Shipwreck	28.9	27.8	0.4	28.3	5.0	4.2	1.9	56.8	17.2	134.7	6.4	1.0	37033.4	3.0	107.0	84.3	0.9
POL19-2	Shipwreck	24.4	25.5	0.3	20.2	4.6	4.5	1.9	53.7	15.2	123.2	5.9	0.9	34579.0	2.8	75.6	79.2	0.8
POL21	Shipwreck	19.1	27.5	0.3	23.0	4.8	2.3	2.0	56.6	16.5	136.0	5.3	1.0	37197.5	3.1	73.0	79.8	0.8
POL22	Shipwreck	15.8	28.9	0.4	25.0	5.3	2.5	2.4	59.9	14.7	99.1	2.8	1.1	31806.2	4.3	85.1	75.2	0.7
SC1	Shipwreck	27.8	26.2	0.4	21.3	5.1	6.3	2.2	53.6	12.7	86.9	3.1	1.0	31142.2	3.8	50.9	73.9	0.7
SC2	Shipwreck	36.2	26.8	0.5	29.8	5.4	8.2	2.1	56.3	13.1	105.6	3.6	1.0	32297.9	3.6	71.1	81.4	0.8
SC3	Shipwreck	40.5	28.4	0.4	26.4	5.5	6.0	2.3	60.5	15.4	106.9	4.1	1.1	35583.8	4.3	56.2	68.5	0.9
SC4	Shipwreck	47.6	28.0	0.3	25.3	5.2	2.1	2.2	58.1	24.0	107.4	5.4	1.1	46441.9	4.2	84.5	23.9	0.9
SC5	Shipwreck	40.7	26.8	0.3	23.9	5.0	3.1	2.0	55.4	16.8	98.3	4.5	1.0	37567.6	3.9	72.0	70.9	0.5
SC7	Shipwreck	13.2	27.2	0.3	26.9	4.9	2.6	2.0	57.0	11.8	69.0	2.2	1.1	30435.3	6.1	61.7	48.9	0.4
SC10	Shipwreck	26.7	28.3	0.3	25.1	5.2	3.1	2.2	59.0	14.3	67.3	2.0	1.0	32160.0	7.6	57.7	44.9	0.5
VIC31	Land	9.2	32.5	0.3	26.1	6.0	2.4	2.3	64.0	14.4	121.3	6.8	1.2	36747.9	4.0	49.9	120.4	0.5
NAK1	Land	6.9	31.6	0.3	23.0	5.5	2.8	2.2	64.1	14.2	117.5	6.7	1.2	38254.0	3.6	48.6	121.4	0.6
NAK4	Land	3.5	31.9	0.3	25.0	5.7	3.3	2.0	65.2	14.2	144.3	7.3	1.1	40375.9	4.0	45.5	134.8	0.6
NAK5	Land	4.9	30.3	0.4	28.0	5.6	3.3	2.1	61.4	15.0	142.6	6.9	1.1	37868.0	3.8	58.1	125.9	0.5
NAK6	Land	9.6	35.0	0.4	30.4	6.4	3.2	2.8	70.5	15.6	146.2	7.0	1.3	41949.4	4.9	47.9	130.4	0.6
NAK7	Land	11.5	29.1	0.3	26.1	5.6	2.1	2.4	57.1	12.1	104.9	3.9	1.1	32947.9	3.9	40.6	78.5	0.5
NAK9	Land	7.8	32.9	0.4	27.7	6.2	2.6	2.4	66.5	16.8	146.3	7.0	1.2	42184.3	4.3	24.4	125.8	0.6
NAK10	Land	5.6	30.0	0.2	16.9	4.4	1.4	1.9	61.1	12.7	102.1	6.2	1.1	35134.8	4.1	37.3	106.1	0.5
NAK15	Land	5.0	34.9	0.3	19.8	4.9	1.6	2.1	71.1	18.6	156.3	2.5	1.2	44299.5	4.2	46.6	74.5	0.6
NAK24	Land	12.1	31.1	0.4	26.0	5.8	3.6	2.5	62.8	14.2	115.6	6.6	1.1	34349.6	4.4	35.9	286.1	0.7
NAK26	Land	9.2	30.6	0.3	27.0	5.7	2.4	2.3	59.8	13.6	112.8	7.4	1.1	36945.0	3.6	41.8	214.1	0.5
NAK27	Land	3.8	32.1	0.3	24.5	5.9	2.9	2.2	65.6	17.7	140.3	7.1	1.2	41713.7	4.1	63.4	132.9	0.6
NAK29	Land	7.5	32.3	0.4	27.5	6.1	2.6	2.2	65.3	14.8	143.2	6.3	1.2	40610.2	3.9	37.0	122.2	0.6

NAK30	Land	8.0	35.3	0.4	28.5	6.8	2.8	2.6	70.5	14.3	130.0	7.8	1.3	40476.8	4.4	69.2	124.9	0.6
NAK31	Land	7.2	37.3	0.4	33.1	7.0	3.0	2.7	75.8	18.0	132.0	5.8	1.3	42322.3	5.1	59.3	108.9	0.7
NAK33	Land	7.8	31.8	0.4	25.4	6.1	2.4	2.5	63.1	11.6	93.4	5.0	1.2	35535.6	3.9	30.7	91.2	0.5
NAK34	Land	9.6	36.4	0.4	29.9	7.0	2.9	3.1	75.1	16.7	107.2	6.6	1.3	37547.0	5.7	59.7	134.8	0.7
<b>Mean</b>		18.6	30.0	0.3	25.9	5.5	3.1	2.3	60.4	14.9	116.8	4.8	1.1	36377.8	3.9	55.4	87.0	0.5
<b>SD</b>		12.5	3.5	0.0	2.8	0.6	1.3	0.3	7.3	2.5	24.3	1.6	0.1	5193.1	0.7	19.7	36.3	0.4
<b>CV (%)</b>		67	12	13	11	11	43	13	12	17	21	34	11	14	18	35	42	74

*Table 1B: Continued geochemical composition of analysed amphorae from Group 1 measured by INAA*

Sample	Site	Sc	Sr	Ta	Tb	Th	Zn	Zr	Al	Ba	Ca	Dy	K	Mn	Na	Ti	V
SGP1	Land	13.8	254.5	0.9	0.8	10.3	139.4	105.8	71444.0	384.6	132923.2	4.2	10150.2	987.5	10849.3	3676.5	79.2
SGP18	Land	15.6	585.0	1.1	0.9	10.7	107.1	110.6	80884.6	515.2	114081.6	4.2	21989.9	1514.5	5130.0	3296.3	113.4
SGP23	Land	10.8	433.3	0.8	0.9	8.3	100.5	90.8	52125.6	379.8	159901.8	3.6	16015.7	983.7	5345.8	2709.5	73.9
SGP27	Land	12.4	250.8	1.0	0.7	10.3	101.9	100.2	64846.8	404.8	91118.3	4.0	22277.9	676.5	6656.1	3443.0	87.4
RES1	Land	14.2	492.7	1.0	0.8	10.4	83.8	85.0	71909.8	513.3	124766.4	4.2	14566.9	842.2	7097.5	3631.1	94.1
RES2	Land	14.4	316.6	1.1	0.8	11.1	107.0	104.0	78774.0	531.0	91429.3	4.3	18165.5	943.8	6381.4	3866.7	89.3
RES3	Land	12.7	259.9	1.0	0.8	10.9	85.6	117.1	64895.2	691.6	93028.0	4.4	19713.8	728.0	6750.5	3247.7	99.0
RES4	Land	13.7	419.4	1.2	0.8	10.3	98.4	93.9	69205.0	704.4	123133.0	4.2	15909.5	885.1	3050.6	3688.6	59.3
RES10	Land	14.2	358.5	1.2	0.9	11.0	103.0	87.6	74869.6	662.0	100430.2	4.9	16455.6	1429.4	4442.8	4648.4	78.0
RES12	Land	14.4	394.1	1.1	0.9	10.4	102.5	97.2	72947.5	633.4	86806.4	4.1	20462.8	1180.0	6400.4	4539.3	100.0
RES13	Land	13.7	285.9	1.0	1.1	11.0	95.0	115.5	68818.3	550.9	84234.4	4.9	16229.3	818.5	4853.3	4351.5	97.6
RES14	Land	14.4	394.4	1.1	1.1	10.2	95.2	114.9	73314.5	405.0	101809.1	4.2	18252.4	1023.2	7086.3	3908.2	112.8
RES15	Land	13.1	244.6	1.1	0.9	10.6	102.3	107.5	70229.3	506.2	105427.9	4.4	17446.2	922.2	4499.5	3725.6	76.3
RES17	Land	12.2	417.1	1.0	0.8	9.6	71.1	118.4	57815.7	583.3	122838.2	4.0	10636.7	795.7	5084.1	3239.4	79.4
RES19	Land	12.8	400.9	1.0	0.8	9.4	104.4	98.1	68651.9	429.0	133016.1	4.2	12166.7	901.0	3364.2	3434.7	76.6
RES20	Land	15.8	328.8	1.2	0.9	11.4	102.6	116.5	80180.7	421.6	75087.5	4.7	19722.5	1138.3	6136.1	4542.1	98.3
RES22	Land	13.8	297.5	1.1	0.9	11.5	101.4	121.1	79608.4	507.3	79947.2	4.6	16989.4	970.6	6603.9	3683.3	98.4
RES23	Land	14.2	161.8	1.2	0.9	12.0	103.9	111.3	74131.9	594.2	71083.9	5.0	22798.4	996.0	7712.0	4238.6	87.2
RES24	Land	12.4	239.9	1.1	1.0	10.6	92.6	84.1	67531.1	551.1	93049.1	4.3	18519.7	755.2	7343.0	3985.2	95.5

RES25	Land	16.6	520.5	1.2	1.1	12.0	95.8	106.2	82486.8	820.3	86029.8	4.9	25591.7	1354.1	4314.7	4049.9	122.5
RES27	Land	15.3	384.0	1.2	1.1	12.3	103.6	121.5	84006.3	347.9	70022.4	4.8	19911.0	752.7	8299.6	4338.2	101.6
RES28	Land	12.9	496.3	1.0	0.9	9.0	83.0	92.1	70323.9	648.2	140654.6	4.1	12002.7	1127.1	3009.9	3582.4	88.1
RES30	Land	15.3	303.7	1.3	0.9	11.8	104.7	103.6	80742.1	507.2	84164.5	5.0	18428.6	1023.4	6469.4	4023.8	85.4
RES32	Land	15.7	324.3	1.2	1.1	11.1	107.8	116.0	81704.4	384.1	83950.8	4.4	15285.0	1323.6	5079.7	3871.1	101.2
RES33	Land	12.9	471.9	1.0	0.7	9.2	86.7	75.6	67693.3	479.1	150204.9	4.0	12799.8	843.4	3433.6	3247.4	92.7
RES35	Land	13.2	246.8	1.3	1.0	11.7	123.3	114.8	84575.2	524.4	80187.3	5.0	21092.0	786.2	8040.9	4128.6	86.6
RAT1	Land	12.9	533.8	1.1	0.8	11.0	96.7	121.9	87760.4	413.4	82094.0	3.9	16859.3	679.7	14545.9	3730.9	88.6
SOK6	Land	12.5	336.7	1.0	0.8	9.0	97.9	111.4	66202.9	511.8	137727.1	4.1	18275.8	790.6	3116.2	2824.0	80.0
VS1	Shipwreck	11.0	471.9	0.8	0.6	7.9	82.8	99.0	55514.4	242.8	90117.3	3.5	10704.1	715.1	15350.1	3141.1	97.7
VS3	Shipwreck	10.8	452.5	0.9	0.6	8.3	76.2	117.5	55397.3	272.7	115741.4	3.3	18511.0	827.1	13235.1	2697.2	106.3
VS4	Shipwreck	10.6	381.9	0.8	0.6	8.1	85.3	90.5	56256.9	217.9	120762.3	3.7	15466.0	694.1	8893.3	2912.5	94.6
VS5	Shipwreck	10.9	476.4	0.8	0.5	7.9	90.4	109.0	55722.0	275.5	69697.6	3.6	10276.6	802.5	11298.6	2941.7	92.5
VS6	Shipwreck	10.2	1151.9	0.8	0.5	7.5	79.1	114.3	53414.0	291.9	151558.8	3.4	16069.5	555.5	7897.3	2831.4	95.8
VS7	Shipwreck	11.2	493.4	0.8	0.6	8.1	84.0	81.1	53429.5	228.4	98340.3	3.5	8055.6	816.9	11925.8	2433.5	94.6
VS9	Shipwreck	10.7	473.5	0.8	0.6	7.8	84.4	99.1	54074.6	274.6	117410.1	3.5	20170.2	742.6	12254.3	2604.8	83.6
VS10	Shipwreck	11.4	360.4	1.0	0.6	9.3	80.8	130.5	60117.8	277.4	99880.5	4.0	17185.2	676.9	20315.6	3717.4	111.1
VS11	Shipwreck	11.2	433.0	0.8	0.7	8.2	88.9	104.9	56458.5	276.0	87382.2	4.0	12281.6	688.4	12059.8	2627.6	83.3
VS13	Shipwreck	11.8	251.4	0.9	0.8	8.8	99.0	101.0	63403.5	229.0	67479.4	4.0	15434.4	827.6	10157.9	2879.1	85.5
VS14	Shipwreck	11.6	415.3	0.9	0.6	8.7	83.7	96.0	62648.9	234.3	95253.7	3.7	15692.5	595.1	8841.1	2683.6	89.4
VS15	Shipwreck	11.4	390.1	0.9	0.6	8.4	84.4	103.1	60474.8	320.0	70318.0	3.7	16315.3	729.9	10758.4	3068.6	109.3
VS16	Shipwreck	10.7	455.8	0.8	0.5	7.7	81.5	127.9	56894.1	283.9	143647.0	3.6	19376.2	649.0	11692.3	2539.7	104.7
VS17	Shipwreck	11.5	525.6	0.8	0.6	8.4	99.2	100.1	61537.4	290.8	120848.8	4.0	13669.8	713.1	8112.8	3361.2	101.6
VS18	Shipwreck	11.2	367.3	0.9	0.6	8.7	83.8	95.4	63460.5	277.8	118993.1	3.7	15511.5	633.6	11458.9	2941.8	82.5
VS19	Shipwreck	11.1	389.1	0.9	0.7	9.1	82.0	108.2	59971.5	250.7	98109.7	4.0	20646.0	671.7	18299.8	2614.1	94.3
VS20	Shipwreck	10.7	624.3	0.8	0.6	7.4	79.7	69.9	56087.9	210.8	186250.6	3.5	18375.1	718.7	8221.9	2582.4	74.7
VS21	Shipwreck	11.6	626.1	0.9	0.7	8.6	91.6	100.5	59535.0	232.6	111477.5	3.9	7650.9	1240.0	8471.9	3023.7	119.9
VS22	Shipwreck	13.3	389.1	1.0	0.7	9.8	103.6	87.8	74263.0	347.3	78465.6	4.0	15648.3	704.4	9087.3	2997.4	106.4
VS24	Shipwreck	10.5	529.9	0.9	0.6	9.8	72.2	97.4	59668.7	250.9	150250.3	4.1	11778.3	758.7	10975.7	3070.5	64.9
VS25	Shipwreck	11.1	603.4	0.9	0.7	7.9	87.2	88.1	56302.9	229.6	119317.8	3.8	9969.1	701.2	9688.8	2809.3	97.1
VS26	Shipwreck	11.2	458.4	0.8	0.7	8.4	80.2	103.5	55404.5	240.8	142800.8	3.6	18040.4	650.8	10647.8	2823.8	89.7
VS27	Shipwreck	10.3	474.3	0.8	0.8	7.7	80.0	92.7	51490.8	187.7	135472.8	3.5	15212.2	625.3	9994.8	3032.7	111.5
VS28	Shipwreck	10.1	424.2	0.7	0.6	7.7	74.6	124.0	53345.9	286.2	119984.4	3.5	12721.9	757.0	11430.8	2710.2	83.3

VS29	Shipwreck	12.6	463.0	0.9	0.8	8.7	94.2	122.9	63552.8	308.6	87157.9	4.1	14541.8	672.6	11321.2	3722.9	108.8
VS30	Shipwreck	12.4	468.6	1.0	0.9	9.2	83.4	129.3	60946.5	296.2	120593.8	4.5	22119.5	900.6	16319.8	3047.7	108.3
VS31	Shipwreck	9.9	1165.8	0.8	0.5	7.0	76.0	87.4	51969.1	285.1	193843.3	3.5	7016.2	671.5	13826.8	2149.3	88.0
VS32	Shipwreck	9.9	1009.0	0.7	0.5	7.2	75.7	91.3	54773.9	219.4	135194.3	3.7	14278.2	675.4	12228.5	2905.2	90.2
POL1	Shipwreck	12.9	405.4	1.2	0.7	10.2	96.8	100.7	69505.0	241.4	120931.2	4.0	17980.0	692.6	9027.1	3739.1	101.0
POL3	Shipwreck	17.9	545.9	0.9	0.8	9.5	108.8	125.0	76818.8	298.8	76024.7	3.9	18379.5	597.2	11138.2	4747.5	133.9
POL4	Shipwreck	12.7	555.7	1.0	0.7	9.5	97.9	80.7	83147.0	250.9	26046.5	5.0	21516.3	511.0	10741.3	4650.6	123.7
POL5	Shipwreck	13.1	490.6	1.0	0.6	9.2	99.6	99.9	66177.5	166.8	124176.1	3.6	17305.4	763.3	7967.8	2643.0	84.2
POL7	Shipwreck	10.6	632.7	0.9	0.6	7.8	82.5	108.8	53672.2	189.7	122121.8	3.6	10943.7	580.1	10671.9	2663.9	80.1
POL8	Shipwreck	13.4	442.1	1.1	0.8	9.5	100.4	73.3	67034.0	231.2	112119.0	3.9	18390.5	832.9	9057.9	3783.2	93.7
POL9	Shipwreck	15.6	336.6	1.2	0.7	11.6	111.0	107.6	78586.0	327.3	79461.0	4.2	20354.8	966.6	10167.2	3985.9	93.3
POL11	Shipwreck	10.2	432.2	0.8	0.7	7.6	81.3	90.0	54706.0	132.6	109252.4	3.6	10369.8	549.2	10148.5	2801.8	84.8
POL14	Shipwreck	12.7	404.8	1.0	0.7	9.8	89.8	101.3	65675.1	243.4	128482.6	3.8	17668.3	741.8	9030.5	3733.4	94.3
POL17	Shipwreck	11.1	499.2	0.9	0.7	9.0	86.3	127.3	57725.8	305.4	135225.2	4.0	14594.9	522.3	9578.3	3334.3	84.3
POL18	Shipwreck	12.8	428.8	1.0	0.7	9.1	95.3	109.5	69028.7	306.6	113470.9	3.4	20152.3	674.5	8565.5	2395.0	115.0
POL19-1	Shipwreck	12.9	683.9	1.0	0.6	8.9	98.7	75.5	63438.6	382.7	150314.3	3.3	17510.8	950.1	10923.5	2901.2	106.1
POL19-2	Shipwreck	12.1	626.6	0.9	0.5	8.3	90.6	80.0	60306.0	287.5	170040.2	3.4	16330.7	948.1	10719.1	4081.5	101.4
POL21	Shipwreck	13.1	605.7	1.0	0.8	8.9	95.7	78.4	66269.4	235.8	130951.1	3.4	14302.7	1028.5	9188.6	2665.7	109.5
POL22	Shipwreck	11.4	602.9	0.9	0.7	9.3	85.8	132.7	58885.3	242.5	117503.7	3.9	15472.2	575.4	10352.3	2582.8	77.0
SC1	Shipwreck	10.7	596.4	0.9	0.7	8.2	133.3	112.1	58877.7	305.6	114363.4	3.7	14649.9	722.4	4316.6	3193.4	85.3
SC2	Shipwreck	11.0	709.8	0.9	0.6	8.5	88.0	127.4	65846.1	3440.9	115844.4	3.8	15229.1	709.5	4674.1	2891.0	101.2
SC3	Shipwreck	12.1	735.0	1.1	0.7	9.3	88.8	146.8	68608.6	340.8	86890.9	3.9	13135.7	749.6	5603.5	3020.2	120.9
SC4	Shipwreck	12.1	1017.8	1.0	0.7	9.2	189.0	116.7	65782.4	372.2	137033.0	4.0	3222.2	808.4	11660.7	3371.3	105.7
SC5	Shipwreck	11.5	649.2	1.0	0.7	8.5	137.7	97.3	63253.6	394.6	112778.2	3.8	14700.3	1024.9	5659.3	3297.8	104.0
SC7	Shipwreck	9.8	487.8	1.1	0.7	7.6	69.9	165.1	55501.4	197.3	114938.6	3.3	12960.5	533.7	5767.8	3258.3	75.7
SC10	Shipwreck	9.3	376.3	1.1	0.7	8.3	79.1	193.2	57766.6	202.9	98873.6	3.8	13517.5	479.7	7812.5	3317.7	90.6
VIC31	Land	13.3	484.5	1.0	0.8	10.0	123.3	123.9	70516.1	386.6	141503.8	4.3	14099.2	805.8	9150.5	3266.8	82.7
NAK1	Land	13.6	450.4	1.0	0.9	9.9	131.0	96.5	71405.2	365.4	130623.2	4.1	20297.7	813.0	5861.6	3425.7	89.0
NAK4	Land	14.7	413.4	1.2	0.7	10.0	144.0	104.2	75125.9	621.5	74630.2	4.1	25237.4	768.6	6773.4	4456.6	88.3
NAK5	Land	13.5	426.9	1.0	0.8	9.5	233.0	108.1	73794.0	461.2	101195.6	3.9	25203.0	841.8	6448.2	3485.7	86.3
NAK6	Land	14.8	412.8	1.2	0.8	11.2	178.7	123.7	75855.0	330.1	90088.7	4.6	24983.9	964.3	6939.5	3696.7	103.8
NAK7	Land	11.8	370.7	1.0	0.8	8.9	132.7	103.2	55474.7	533.9	142315.2	4.2	19398.9	843.9	5578.6	2623.5	65.5
NAK9	Land	14.6	450.2	1.2	0.9	10.5	147.2	109.5	77917.3	504.7	107639.8	4.6	20803.1	1003.8	6788.7	3483.3	112.6

NAK10	Land	12.5	316.7	1.0	0.8	9.7	112.5	96.1	62443.4	302.4	125439.3	3.9	20058.9	748.7	6044.7	2946.4	79.9	
NAK15	Land	15.7	508.4	1.3	0.9	11.0	159.0	93.2	79846.5	233.5	104268.8	4.1	20554.7	1047.8	8511.0	3683.6	105.8	
NAK24	Land	12.4	494.9	1.0	0.7	9.9	109.3	139.1	62099.7	360.0	140452.4	3.9	20196.4	748.7	5813.4	2937.2	93.7	
NAK26	Land	13.1	541.8	1.0	0.8	9.3	177.3	106.7	63937.6	415.9	139682.6	4.1	19292.5	820.3	7371.5	3538.4	83.0	
NAK27	Land	14.7	370.9	1.1	0.6	10.3	164.4	99.7	72262.9	310.0	82164.7	4.4	23254.8	1285.3	6968.2	3146.1	75.2	
NAK29	Land	14.3	415.7	1.1	0.9	10.3	165.0	129.2	75011.0	465.4	101299.8	4.2	24146.8	1004.4	6583.1	3569.3	107.4	
NAK30	Land	14.4	382.7	1.2	0.7	11.3	193.8	101.8	74292.4	495.2	101488.5	4.9	19694.3	967.8	7654.4	3680.5	87.5	
NAK31	Land	15.5	550.0	1.3	0.7	12.0	144.1	129.1	74958.3	492.2	102481.9	4.9	21201.0	1156.7	6762.0	3530.5	85.4	
NAK33	Land	12.5	322.4	1.0	0.9	10.1	127.6	106.0	59254.9	428.0	123163.5	4.3	20952.9	687.5	5986.3	2986.7	62.2	
NAK34	Land	13.9	411.9	1.2	1.0	11.7	151.8	140.4	72324.2	486.3	79987.1	5.0	25484.5	1259.6	8285.6	3917.1	99.3	
<b>Mean</b>		12.6	468.1	1.0	0.8	9.5	104.9	107.1	66283.4	402.4	110850.1	4.0	16894.5	834.9	8485.9	3346.9	93.5	
<b>SD</b>		1.8	172.8	0.1	0.1	1.3	30.4	19.2	9259.0	345.4	27941.9	0.5	4405.3	211.3	3268.6	589.3	14.1	
<b>CV (%)</b>		14	37	14	19	14	29	18	14	86	25	11	26	25	39	18	15	

*Table 2A: Geochemical composition of analysed amphorae from Group 2 measured by INAA*

Sample	Site	As	La	Lu	Nd	Sm	U	Yb	Ce	Co	Cr	Cs	Eu	Fe	Hf	Ni	Rb	Sb	Sc	Sr
SGP2	Land	10.1	25.0	0.3	20.2	5.0	2.3	2.4	50.8	29.9	409.7	5.4	1.1	44754.0	3.5	261.1	106.1	0.5	16.1	393.2
SGP3	Land	12.4	27.0	0.3	24.2	4.7	2.1	2.1	53.5	34.2	328.5	7.4	1.0	41767.2	3.7	377.9	89.2	0.7	13.3	249.1
SGP4	Land	10.5	22.7	0.3	19.8	4.6	1.6	2.4	49.5	30.2	347.9	14.1	1.1	51125.4	3.7	277.8	91.3	0.5	19.5	364.6
SGP5	Land	7.9	23.4	0.3	17.7	4.7	1.6	2.1	47.3	25.9	445.1	5.8	1.0	42805.1	3.4	233.6	109.1	0.6	15.3	318.8
SGP9	Land	14.1	25.3	0.3	20.6	5.0	3.2	2.4	49.7	26.2	404.2	6.0	1.1	45374.8	3.4	229.0	107.0	0.6	16.2	407.1
SGP10	Land	13.0	24.3	0.3	25.5	4.8	2.1	2.2	48.4	24.3	384.0	4.8	1.0	44130.6	3.4	229.7	96.3	0.6	15.1	348.8
SGP11	Land	8.2	26.5	0.3	20.8	5.3	2.5	2.5	53.1	24.9	486.2	6.6	1.2	44474.1	3.9	228.0	119.8	0.6	16.1	389.3
RAT3	Land	5.4	26.8	0.4	22.8	5.3	2.4	2.3	53.8	29.4	458.4	6.6	1.2	49013.5	3.8	248.5	93.6	0.5	17.6	407.3
RAT5	Land	8.4	22.9	0.3	20.0	4.5	1.8	2.2	44.8	25.7	440.0	5.2	1.0	40294.7	3.1	203.2	99.1	0.5	14.6	311.6
RAT6	Land	8.2	29.0	0.4	25.0	5.6	2.5	2.6	60.6	30.5	429.4	5.4	1.1	52149.1	4.1	287.5	96.9	0.5	18.4	278.5
RAT7	Land	5.6	24.5	0.3	21.6	4.8	2.0	2.1	49.1	25.9	478.0	5.8	1.0	42760.5	3.8	230.6	93.5	0.5	15.1	320.7
ZEM2	Land	1.8	24.7	0.3	20.8	4.8	2.1	2.2	49.4	25.1	487.2	6.1	1.0	43738.2	3.5	245.8	180.7	0.3	15.6	379.7
CG6	Land	0.0	28.0	0.3	24.4	5.3	2.2	2.8	54.3	29.0	498.3	5.1	1.1	48022.6	3.9	296.0	152.6	0.3	17.7	389.7

SOK3	Land	3.9	28.7	0.4	24.7	5.6	2.3	2.4	56.4	30.1	471.0	2.3	1.2	51230.1	3.8	228.4	56.4	0.5	19.0	305.2
SOK4	Land	4.5	27.9	0.4	24.4	5.4	2.2	2.5	56.5	25.9	504.4	2.1	1.2	47641.1	4.5	242.2	54.2	0.0	17.2	0.0
SOK5	Land	4.6	29.1	0.4	25.2	5.7	2.0	2.2	58.2	32.8	495.4	1.6	1.2	52495.3	4.0	266.4	48.8	0.0	19.3	208.2
SOK7	Land	4.6	26.8	0.4	23.8	5.2	1.8	2.3	53.8	28.7	448.9	5.5	1.1	47158.2	3.8	248.8	106.3	0.5	17.3	293.7
SOK9	Land	5.1	27.2	0.3	24.9	5.4	1.6	2.3	54.4	29.1	494.0	2.4	1.2	47114.6	4.0	252.9	61.9	0.5	17.1	318.0
SOK10	Land	6.6	31.1	0.4	28.2	6.1	2.5	2.6	66.3	33.2	475.0	3.8	1.3	54796.6	4.6	297.3	71.8	0.0	19.5	317.0
SOK11	Land	3.9	29.0	0.4	26.6	5.7	2.6	2.5	56.6	29.4	464.4	1.9	1.2	50896.2	3.8	254.7	52.5	0.0	18.9	340.2
SOK13	Land	11.1	28.7	0.4	27.2	5.6	2.6	2.4	60.6	30.0	419.2	3.7	1.1	51281.6	4.4	306.7	92.4	0.0	18.0	128.6
GN2	Shipwreck	69.0	27.8	0.4	26.3	5.5	2.7	2.6	57.4	38.9	341.0	3.1	1.2	59050.0	3.8	235.3	74.8	1.1	20.1	274.9
GN3	Shipwreck	44.0	24.8	0.3	22.9	4.7	2.4	2.5	53.8	38.3	323.4	6.1	1.2	58079.4	4.7	363.8	87.5	3.2	19.3	181.9
GN4	Shipwreck	83.2	27.3	0.4	24.2	5.1	2.8	2.2	53.0	38.9	171.1	3.1	1.1	44995.7	2.9	180.7	52.4	0.8	15.3	1311.1
GN6	Shipwreck	39.0	28.3	0.3	26.9	5.3	2.5	2.3	54.5	33.6	177.6	3.4	1.1	41978.3	3.0	157.3	61.9	0.8	15.7	1002.5
POL19	Shipwreck	39.8	21.7	0.4	19.7	4.4	5.0	2.1	46.3	24.5	470.7	4.9	0.9	47155.2	3.6	320.6	63.4	1.3	16.2	319.0
ZIR16	Shipwreck	97.6	23.4	0.3	19.7	4.5	2.6	2.1	48.8	27.7	276.1	1.1	0.9	54066.1	2.9	248.2	34.6	0.9	16.4	502.3
VIC2	Land	6.8	24.8	0.3	25.0	4.9	2.2	2.3	50.7	25.4	438.5	5.0	1.0	45387.2	3.5	235.7	103.2	0.4	16.4	228.4
VIC3	Land	3.4	24.9	0.3	21.8	5.0	2.5	2.6	50.2	22.6	463.8	5.2	1.0	44474.8	3.8	203.5	100.0	0.5	16.4	278.9
VIC4	Land	4.5	24.8	0.3	22.6	4.8	2.1	2.1	49.7	22.2	494.6	4.5	1.0	47258.8	3.9	217.2	88.3	0.5	17.2	247.0
VIC5	Land	4.2	26.0	0.3	22.9	5.0	2.5	2.3	51.8	24.1	450.1	6.7	1.1	47342.5	3.7	236.5	128.4	0.6	17.7	307.0
VIC6	Land	4.4	23.3	0.3	19.9	4.6	2.3	2.1	48.0	25.7	469.2	5.8	1.0	45988.1	3.6	182.3	105.8	0.6	16.5	258.8
VIC7	Land	8.3	24.1	0.3	19.1	4.8	2.4	2.3	47.8	22.1	479.9	6.0	1.0	44779.2	3.7	227.0	113.8	0.5	16.3	283.7
VIC8	Land	2.0	25.1	0.3	21.8	4.8	2.3	2.1	50.4	22.4	455.6	6.3	1.0	45717.8	3.5	210.4	82.7	0.4	17.1	348.3
VIC9	Land	3.4	25.4	0.3	21.6	4.9	2.8	2.2	49.4	23.3	417.4	6.1	1.1	44658.8	3.4	215.7	99.7	0.5	16.4	359.3
VIC10	Land	3.9	26.3	0.3	22.7	5.1	2.6	2.6	51.3	28.0	430.5	6.0	1.0	45777.4	3.6	205.5	113.5	0.5	16.7	345.7
VIC11	Land	4.9	21.8	0.3	21.2	4.4	2.9	2.0	45.2	23.9	443.0	5.6	0.9	46086.7	3.7	217.8	108.4	0.6	16.8	266.4
VIC12	Land	3.5	26.7	0.3	22.7	5.2	2.5	2.2	53.0	27.2	470.0	6.0	1.1	47022.4	3.8	244.3	111.7	0.5	16.9	263.9
VIC13	Land	4.8	25.0	0.3	22.2	5.0	2.3	2.3	50.2	25.5	436.5	5.7	1.0	43824.2	3.6	235.0	113.0	0.5	16.2	276.9
VIC14	Land	3.3	26.3	0.3	22.6	5.1	2.4	2.4	51.8	27.2	414.2	6.1	1.1	46947.5	3.6	229.0	109.2	0.6	17.1	257.4
VIC15	Land	6.1	28.6	0.4	24.0	5.7	2.7	2.5	57.4	29.8	533.7	3.9	1.2	50321.8	4.2	258.4	78.4	0.5	17.3	137.0
VIC16	Land	4.4	23.7	0.3	21.5	4.6	2.1	2.2	47.6	24.4	437.8	5.3	1.0	41482.9	3.4	212.5	104.9	0.4	15.2	276.1
VIC18	Land	4.0	23.2	0.3	21.8	4.4	2.3	1.9	45.5	24.7	400.3	5.0	0.9	39046.7	3.1	209.0	94.8	0.5	14.2	334.6
VIC19	Land	3.3	25.6	0.3	25.6	5.2	2.3	2.4	51.6	28.1	458.2	5.5	1.1	48011.9	3.8	230.1	105.7	0.5	16.9	313.8
VIC20	Land	3.4	26.7	0.4	23.3	5.3	2.6	2.7	54.6	29.4	496.5	5.5	1.1	49976.9	3.8	253.6	106.4	0.5	17.8	335.6
VIC22	Land	3.2	25.1	0.3	24.9	4.9	2.2	2.4	49.4	27.8	441.5	5.8	1.0	43206.5	3.6	258.0	108.9	0.5	15.8	310.6

VIC23	Land	3.6	21.3	0.4	19.3	4.3	2.8	2.2	42.5	20.4	433.1	5.6	0.9	39432.0	3.7	186.4	113.9	0.4	14.7	223.7
VIC24	Land	6.8	26.4	0.3	24.3	5.1	2.6	2.3	50.3	16.1	428.7	2.6	1.0	42542.6	3.4	113.2	63.2	0.4	15.4	259.3
VIC25	Land	4.6	24.9	0.3	20.7	4.9	1.8	2.6	49.9	26.4	451.3	5.8	1.0	43347.4	3.7	231.8	110.7	0.4	15.9	307.7
VIC26	Land	7.8	26.0	0.4	24.2	5.1	2.4	2.3	51.7	28.0	453.7	5.5	1.1	45519.2	3.7	240.3	92.6	0.6	16.2	286.1
VIC27	Land	5.8	26.3	0.3	24.1	5.4	1.9	2.2	53.9	26.3	459.4	3.7	1.1	48190.3	3.7	178.6	73.0	0.5	17.3	329.4
VIC28	Land	4.9	23.8	0.3	21.0	5.0	2.3	2.2	50.4	28.6	407.1	4.6	1.1	45064.0	3.3	162.6	90.4	0.4	16.6	200.5
VIC29	Land	3.1	22.7	0.3	16.9	4.5	2.4	1.9	47.2	24.9	437.3	5.5	1.0	42124.0	3.6	151.7	101.0	0.5	15.4	305.2
VIC30	Land	3.9	26.5	0.3	24.1	5.2	2.4	2.3	53.4	22.6	479.3	4.8	1.1	45053.6	3.7	132.5	78.5	0.4	16.3	308.3
VIC32	Land	7.5	26.2	0.4	23.3	5.3	2.6	2.3	55.8	28.6	409.6	5.8	1.0	47011.8	3.8	171.9	115.7	0.5	16.8	260.6
NAK3	Land	2.3	22.8	0.3	18.8	4.1	1.4	2.2	47.9	25.7	454.0	6.1	1.0	44753.4	3.7	193.0	108.9	0.5	16.3	385.0
<b>Mean</b>		11.7	25.6	0.3	22.7	5.0	2.4	2.3	51.8	27.4	431.7	5.1	1.1	46583.9	3.7	232.1	94.3	0.5	16.7	327.8
<b>SD</b>		19.4	2.1	0.0	2.5	0.4	0.5	0.2	4.3	4.3	69.4	1.9	0.1	4186.3	0.4	49.1	25.5	0.4	1.4	181.1
<b>CV (%)</b>		166	8	8	11	8	21	8	8	16	16	37	8	9	10	21	27	77	8	55

*Table 2B: Continued geochemical composition of analysed amphorae from Group 2 measured by INAA*

Sample	Site	Ta	Tb	Th	Zn	Zr	Al	Ba	Ca	Dy	K	Mn	Na	Ti	V
SGP2	Land	0.8	0.9	7.9	118.3	108.0	63346.6	335.7	95598.9	4.0	21823.4	1028.6	9656.1	3626.2	110.2
SGP3	Land	0.7	0.7	9.5	81.4	99.4	59258.6	337.7	124604.6	3.5	17953.1	1142.7	2391.7	2622.4	97.4
SGP4	Land	0.7	0.9	7.5	97.9	102.3	69888.4	343.0	88163.1	3.8	15921.0	1033.3	8067.7	4638.5	114.5
SGP5	Land	0.8	0.6	7.3	96.0	122.2	56171.9	373.0	98970.5	3.8	20510.1	971.0	7701.1	3111.4	99.2
SGP9	Land	0.7	0.6	7.9	123.0	105.8	63932.5	358.7	102320.2	4.0	20115.3	941.6	7684.2	3470.7	119.7
SGP10	Land	0.7	0.7	7.2	105.6	92.1	55633.8	397.5	113835.0	3.7	18088.8	1029.5	6402.6	2809.8	83.9
SGP11	Land	0.8	1.0	7.8	83.6	117.7	64122.9	423.4	96823.6	4.6	18748.0	1130.8	10212.0	3339.2	116.5
RAT3	Land	0.8	0.6	8.7	109.2	98.6	70744.4	433.8	93030.3	4.3	16747.1	942.5	10341.0	3914.8	113.0
RAT5	Land	0.7	0.5	7.0	108.6	99.5	61137.7	325.2	102958.5	3.7	22027.4	817.8	8079.6	3489.0	97.1
RAT6	Land	1.0	0.8	10.1	112.8	110.2	75062.9	504.5	77471.1	4.5	18194.3	1121.3	9786.9	4230.9	136.2
RAT7	Land	0.8	0.8	7.6	104.6	82.2	61472.8	407.6	97034.5	3.8	17814.8	984.4	8992.2	3910.2	89.4
ZEM2	Land	0.8	0.6	7.6	93.3	74.0	67243.7	430.9	95776.8	4.1	17417.9	817.4	12138.7	4226.0	109.8
CG6	Land	0.9	0.7	8.6	87.3	97.3	65087.7	337.4	105655.9	4.5	14810.6	909.4	11926.6	3988.7	140.9

SOK3	Land	0.8	0.7	9.0	149.2	89.8	77202.7	712.6	92934.8	4.9	14649.2	970.3	4914.7	4336.8	109.9
SOK4	Land	0.8	0.7	8.6	167.2	102.9	70884.2	543.5	87839.6	4.2	15082.7	835.6	7122.9	4200.9	90.8
SOK5	Land	0.9	0.7	9.1	166.3	104.8	81073.3	604.9	67513.5	4.6	14366.3	1207.6	5918.6	4104.2	101.6
SOK7	Land	0.8	0.7	8.3	116.1	102.0	65064.9	477.8	83551.6	4.1	20490.1	858.9	8815.1	3242.9	103.4
SOK9	Land	0.8	0.7	8.4	106.1	85.2	67099.1	465.9	91379.0	4.5	15064.5	916.6	7565.8	3508.1	112.6
SOK10	Land	1.1	0.7	10.8	148.2	121.2	77827.1	570.9	71205.9	4.7	16727.4	1059.1	8269.6	4290.3	110.2
SOK11	Land	0.9	0.7	8.9	142.8	125.9	71509.6	692.7	92848.3	4.5	14904.2	980.6	4769.7	4248.2	108.0
SOK13	Land	0.9	0.7	10.1	156.1	97.1	70225.0	659.0	57689.8	4.4	20758.4	957.2	8870.9	3803.5	101.3
GN2	Shipwreck	0.8	0.7	9.5	118.9	95.0	74737.6	235.2	67017.8	4.8	17184.9	1172.6	9647.1	4186.5	143.2
GN3	Shipwreck	1.0	0.6	9.7	103.5	122.4	80119.3	268.6	75453.0	3.8	18806.8	757.3	7017.4	4305.7	116.4
GN4	Shipwreck	0.7	0.7	8.3	101.7	92.7	64765.1	145.3	129297.4	4.3	12030.7	1347.2	5566.6	3548.6	121.8
GN6	Shipwreck	0.8	0.7	8.5	103.8	102.2	65397.3	190.4	118089.2	4.0	13660.0	1093.1	6707.3	3175.9	126.1
POL19	Shipwreck	0.8	0.8	7.0	100.9	107.5	59806.1	129.1	92719.2	3.0	13096.2	453.1	9073.6	3923.5	119.1
ZIR16	Shipwreck	0.8	0.6	8.0	108.7	79.6	65284.5	190.9	94280.0	3.7	9842.2	791.0	7211.6	3271.2	141.5
VIC2	Land	0.8	0.6	8.1	130.6	83.6	69136.3	277.7	76803.9	3.9	19905.3	847.6	8681.1	3802.9	106.6
VIC3	Land	0.8	0.9	8.1	141.1	102.5	68002.4	292.3	77493.3	4.2	20717.7	706.3	9105.5	3612.7	116.5
VIC4	Land	0.8	0.7	8.4	174.1	107.0	62357.4	368.8	74425.4	4.0	21965.4	692.1	8905.4	4115.3	111.2
VIC5	Land	0.9	0.9	8.3	128.3	98.1	68939.3	405.7	80806.1	4.2	22160.9	748.6	8536.3	4022.4	119.9
VIC6	Land	0.8	0.6	7.9	139.7	99.0	70118.0	384.4	75651.4	3.5	20952.2	740.3	9361.5	3876.8	99.3
VIC7	Land	0.8	0.7	7.9	107.2	85.3	68454.2	444.3	57735.0	3.9	21966.4	673.4	9342.9	3814.0	106.9
VIC8	Land	0.8	0.8	7.9	81.6	85.4	77794.8	363.5	87755.8	3.9	9935.6	706.4	12992.0	3617.2	126.9
VIC9	Land	0.7	0.9	7.7	212.7	95.8	67477.9	349.9	93726.5	4.0	17307.8	786.8	9554.3	3297.0	109.7
VIC10	Land	0.8	0.9	8.2	141.4	118.0	67418.5	324.6	88189.5	4.1	21419.6	900.3	10966.0	3734.3	121.1
VIC11	Land	0.8	0.8	8.1	178.6	96.9	70245.1	302.5	59322.0	3.4	21382.3	708.5	7759.3	3707.4	103.0
VIC12	Land	0.8	0.9	8.2	170.8	97.3	65868.5	350.0	77767.1	4.2	21547.2	811.8	8796.6	4278.3	120.3
VIC13	Land	0.7	0.6	7.8	132.8	88.8	64985.5	296.7	79520.1	3.8	24929.9	838.5	8904.7	4367.8	113.9
VIC14	Land	0.8	0.8	8.2	247.6	96.8	70765.3	351.5	80250.1	4.2	21002.6	847.1	8684.3	3485.5	110.3
VIC15	Land	0.8	0.8	9.0	186.9	110.0	71451.4	344.8	50632.3	4.8	17153.8	975.6	8343.7	4590.3	99.6
VIC16	Land	0.7	0.8	7.6	197.1	84.0	61926.6	292.0	88315.4	3.6	18655.0	801.1	9515.9	3253.2	111.1
VIC18	Land	0.7	0.8	6.8	191.9	76.2	60681.6	369.5	106063.9	3.6	17512.6	1113.9	9254.9	3130.8	98.8
VIC19	Land	0.8	1.0	8.3	153.8	95.6	69162.6	325.4	83944.1	4.3	21207.0	1028.1	8226.5	4003.7	111.7
VIC20	Land	0.9	0.9	8.8	120.1	95.1	69346.8	336.4	76296.4	4.4	20319.7	868.1	8952.5	4251.3	117.2
VIC22	Land	0.7	0.6	7.7	160.8	107.1	66571.6	323.7	80081.5	3.8	22513.6	879.1	9207.2	3355.6	103.4

VIC23	Land	0.8	0.9	7.1	74.9	68.7	57181.5	326.4	61893.5	3.2	28098.4	630.4	9817.6	4033.8	90.2
VIC24	Land	0.7	0.7	7.6	679.3	83.1	68065.8	476.9	52643.9	4.3	18426.6	506.4	7247.9	4197.2	78.1
VIC25	Land	0.8	0.8	8.0	101.5	81.8	60834.8	399.6	72055.8	3.6	22208.0	890.1	8746.9	3583.0	112.5
VIC26	Land	0.7	1.1	8.0	143.5	85.8	65703.2	324.4	97140.1	3.9	17296.4	891.7	7927.0	3805.1	102.4
VIC27	Land	0.9	0.6	8.4	220.8	102.7	65418.9	325.4	83477.4	4.3	13338.6	841.4	7102.1	3938.1	105.7
VIC28	Land	0.8	0.9	7.9	256.5	77.5	68256.8	254.0	65558.5	3.9	18802.6	1306.1	9903.6	3936.6	113.8
VIC29	Land	0.8	0.5	7.6	157.6	114.9	60539.1	245.6	84332.3	3.6	21745.9	723.8	9536.0	3405.4	100.1
VIC30	Land	0.9	0.5	8.1	158.7	64.6	65850.6	365.5	107126.6	4.2	16136.3	782.7	8076.3	3909.7	124.6
VIC32	Land	0.9	0.6	9.0	116.6	109.9	66452.9	316.3	78614.3	3.7	22194.0	951.6	11240.2	3523.1	125.8
NAK3	Land	0.8	0.6	7.8	110.4	92.8	65367.4	195.1	68971.5	3.7	22994.7	747.5	8508.6	3451.7	100.8
<b>Mean</b>		0.8	0.7	8.2	145.1	97.2	67115.6	368.4	85368.9	4.0	18582.7	896.7	8536.6	3779.0	110.6
<b>SD</b>		0.1	0.1	0.8	83.5	13.7	5606.4	121.9	17087.1	0.4	3617.0	178.7	1812.4	437.8	13.4
<b>CV (%)</b>		9	19	10	58	14	8	33	20	10	19	20	21	12	12

*Table 3A: Geochemical composition of analysed amphorae from Group 3 measured by INAA*

Sample	Site	As	La	Lu	Nd	Sm	U	Yb	Ce	Co	Cr	Cs	Eu	Fe	Hf	Ni	Rb	Sb	Sc
SGP6	Land	17.5	47.6	0.5	39.0	8.4	3.6	3.4	99.0	26.2	310.2	9.6	1.8	52769.6	7.5	189.9	123.8	1.6	17.7
SGP19	Land	8.9	45.6	0.4	36.1	8.3	2.6	3.9	96.9	18.5	138.7	10.4	1.6	44357.0	7.3	76.0	146.3	1.0	15.6
SGP21	Land	16.2	50.2	0.5	40.8	8.8	3.3	3.5	100.3	25.2	291.8	9.8	1.8	54229.7	7.2	143.9	131.0	1.8	18.1
RAT2	Land	16.9	42.9	0.4	33.5	6.5	5.9	3.1	109.2	15.9	59.2	11.9	1.2	39174.6	8.3	12.3	164.0	1.0	10.0
STI1	Land	14.4	61.9	0.6	55.8	10.6	2.8	4.5	119.9	27.0	328.6	8.1	2.2	55575.5	9.3	202.3	95.0	1.8	18.9
STI2	Land	8.3	52.3	0.6	44.3	8.7	3.1	4.0	103.8	23.4	337.4	8.3	1.7	50347.5	10.2	164.4	109.3	1.3	16.7
CG3	Land	11.0	34.7	0.4	30.9	6.1	1.9	2.6	75.8	29.0	318.8	6.6	1.3	52298.0	5.3	230.0	108.3	1.1	18.5
CG5	Land	11.4	35.3	0.4	28.4	6.3	2.4	2.8	75.5	27.8	315.9	7.1	1.3	52096.5	5.3	234.6	112.2	0.8	18.8
ZIR5	Shipwreck	64.5	43.7	0.5	40.9	7.8	3.0	3.4	91.6	23.3	265.4	1.2	1.5	48418.1	9.1	139.7	30.8	3.2	13.8
ZIR6	Shipwreck	22.9	40.8	0.4	32.8	6.9	2.8	3.0	81.0	19.4	252.2	5.0	1.3	39109.3	7.9	108.1	71.9	1.2	13.3
ZIR9	Shipwreck	52.4	46.5	0.5	39.4	8.1	2.7	3.4	92.6	25.5	304.0	4.1	1.6	48906.4	8.0	201.1	63.3	2.1	16.0
ZIR11	Shipwreck	15.4	43.3	0.4	38.2	7.4	2.8	3.1	86.4	24.6	318.7	3.3	1.5	45911.4	9.1	171.3	57.6	1.4	15.1
ZIR17	Shipwreck	49.4	42.7	0.6	39.0	8.2	13.8	3.4	87.8	23.4	298.6	4.7	1.5	45235.2	9.4	132.7	70.2	3.3	14.7

ZIR18	Shipwreck	60.0	39.7	0.5	37.2	7.2	3.8	3.2	80.5	28.3	319.8	3.2	1.4	48279.3	7.1	199.6	59.7	1.8	17.1
ZIR22	Shipwreck	31.1	50.7	0.5	40.1	9.1	7.2	3.3	97.0	24.9	258.2	7.0	1.8	50655.7	6.4	161.3	96.6	3.1	16.7
<b>Mean</b>		26.7	45.2	0.5	38.4	7.9	4.1	3.4	93.2	24.2	274.5	6.7	1.6	48490.9	7.8	157.8	96.0	1.8	16.1
<b>SD</b>		19.7	6.9	0.1	6.4	1.2	3.0	0.5	12.5	3.7	77.1	3.1	0.3	4974.4	1.5	59.4	37.0	0.8	2.4
<b>CV (%)</b>		74	15	12	17	15	73	14	13	15	28	46	17	10	19	38	38	47	15

*Table 3B: Continued geochemical composition of analysed amphorae from Group 3 measured by INAA*

Sample	Site	Sr	Ta	Tb	Th	Zn	Zr	Al	Ba	Ca	Dy	K	Mn	Na	Ti	V
SGP6	Land	113.7	1.3	1.1	15.3	124.8	200.5	86554.0	400.7	34990.0	5.9	19389.3	1172.1	5312.5	4378.7	156.7
SGP19	Land	191.8	1.5	1.3	15.9	105.4	203.4	82107.2	513.0	38286.4	6.0	23595.8	717.9	9651.6	4488.4	106.3
SGP21	Land	169.9	1.5	1.1	15.8	121.6	152.0	88565.6	451.7	30337.8	6.3	21324.9	1129.8	5087.8	5043.0	157.4
RAT2	Land	86.1	2.3	0.8	21.1	70.8	264.4	87324.4	383.1	4096.5	4.6	19172.0	998.0	10341.2	3931.2	108.8
STI1	Land	66.3	1.6	1.3	20.8	137.7	233.7	89339.9	311.6	28082.9	7.7	14599.9	1275.0	4224.7	5507.7	130.0
STI2	Land	96.9	1.5	1.4	17.6	130.1	272.0	79507.3	375.3	19596.3	6.7	15585.3	1150.3	5695.4	5153.0	107.6
CG3	Land	252.8	1.1	0.8	12.2	126.9	143.1	76673.1	382.6	70293.9	4.9	20156.0	1145.0	6320.0	4512.6	132.9
CG5	Land	201.3	1.2	1.1	12.3	133.5	136.4	79625.6	343.9	69038.0	5.0	20705.6	1100.8	6526.9	4665.6	119.9
ZIR5	Shipwreck	44.1	1.4	1.3	15.6	107.4	247.6	74700.0	119.3	15662.7	5.5	7223.1	637.0	9318.0	4749.4	82.6
ZIR6	Shipwreck	256.8	1.1	0.9	13.1	90.5	232.8	69368.0	212.8	53363.8	4.9	12378.9	955.3	8172.9	4651.8	101.6
ZIR9	Shipwreck	179.4	1.3	1.2	15.4	115.3	225.1	78685.0	246.2	35875.0	5.6	11150.9	979.3	8629.7	5309.8	123.9
ZIR11	Shipwreck	228.8	1.4	1.1	15.2	113.6	209.7	72278.9	189.7	49925.6	5.2	10184.3	1096.6	9477.1	4236.2	119.1
ZIR17	Shipwreck	125.7	1.3	1.0	14.6	104.6	304.7	77009.1	269.3	29717.3	5.2	12935.6	864.1	9435.3	4738.9	109.6
ZIR18	Shipwreck	110.5	1.2	1.1	13.7	119.8	171.4	79080.5	230.3	44644.7	5.4	16108.4	869.2	10835.3	4706.0	129.6
ZIR22	Shipwreck	194.0	1.4	1.4	15.8	117.5	180.0	93000.3	336.3	52303.1	6.0	14438.3	1063.4	7540.7	5028.1	148.8
<b>Mean</b>		154.5	1.4	1.1	15.6	114.6	211.8	80921.3	317.7	38414.3	5.7	15929.9	1010.2	7771.3	4740.0	122.3
<b>SD</b>		67.6	0.3	0.2	2.6	17.3	49.4	6769.9	106.1	18626.2	0.8	4693.4	176.7	2110.2	416.4	21.0
<b>CV (%)</b>		44	21	17	17	15	23	8	33	48	14	29	17	27	9	17

*Table 4A: Geochemical composition of analysed amphorae from Group 4 measured by INAA*

Sample	Site	As	La	Lu	Nd	Sm	U	Yb	Ce	Co	Cr	Cs	Eu	Fe	Hf	Ni	Rb	Sb	Sc
SGP17	Land	13.0	30.6	0.4	24.9	5.4	2.4	2.7	59.3	33.8	276.9	8.1	1.2	52977.6	3.1	225.4	135.2	0.7	20.2
GN1	Shipwreck	104.4	29.3	0.4	27.7	5.8	8.3	2.2	57.1	48.3	261.0	3.9	1.1	43705.4	3.3	235.3	63.5	0.0	18.1

*Table 4B: Continued geochemical composition of analysed amphorae from Group 4 measured by INAA*

Sample	Site	Sr	Ta	Tb	Th	Zn	Zr	Al	Ba	Ca	Dy	K	Mn	Na	Ti	V
SGP17	Land	450.1	0.8	0.7	9.6	115.5	98.1	80520.9	444.6	109868.4	4.0	24924.3	1221.8	3609.0	3977.3	152.9
GN1	Shipwreck	1113.0	0.8	0.6	9.0	109.5	111.3	70887.4	200.3	105712.5	4.2	14161.5	664.7	5765.0	3867.7	168.1

**Appendix 2:** Results of the t-test in Fabric group 1 and 3, with standard alpha level at 0.05, following reporting: t (degrees of freedom) = the t statistic, p = value, where t = t statistics, df = degrees of freedom depending on sample size and t-test performed, p = probability. (e = standard scientific notation for powers of 10, of example p = 3.751e-10 meaning, possibly value is 3.751 x 10<sup>-10</sup> and is significantly lower than alpha and null hypothesis is rejected: the mean value of specific element in marine and terrestrial samples is not the same)

Element	Fabric 1	Fabric 3
Al	t (88.66) = -7.04, p = 3.3751e-10	t (9.93) = -1.79, p = 0.01
As	t (67.83) = 7.90, p = 3.35e-11	t (6.38) = 3.97, p = 0.006
Ba	t (54.97) = -2.26, p = 0.02	t (12.40) = -4.92, p = 0.0003
Ca	t (91.54) = 1.27, p = 0.20	t (11.74) = 0.34, p = 0.73
Ce	t (83.50) = -10.74, p < 2.2e-16	t (9.39) = -1.59, p = 0.14
Co	t (91.47) = -1.54, p = 0.12	t (11.48) = 0.03, p = 0.96
Cr	t (91.07) = -3.93, p = 0.00016	t (8.21) = 0.66, p = 0.52
Cs	t (88.12) = -4.91, p = 4.164e-06	t (12.71) = -5.34, p = 0.0001
Dy	t (87.32) = -8.34, p = 9.615e-13	t (8.73) = -1.20, p = 0.25
Eu	t (88.26) = -12.79, p 2.2e-16	t (9.55) = -0.65, p = 0.52
Fe	t (91.74) = -6.53, p = 3.447e-09	t (12.36) = -1.42, p = 0.17

Hf	t (84.80) = -3.70, p = 0.00038	t (12.11) = 0.78, p = 0.44
K	t (91.32) = -4.89, p = 4.154e-06	t (12.79) = -4.78, p = 0.0003
La	t (82.06) = -12.59, p < 2.2e-16	t (9.6) = -0.69, p = 0.50
Lu	t (88.97) = -2.33, p = 0.02	t (12.98) = 0.01, p = 0.98
Mn	t (79.01) = -6.01, p = 5.357e-08	t (12.95) = -1.95, p = 0.07
Na	t (82.10) = 7.46, p = 6.514e-11	t (10.39) = 2.75, p = 0.01
Nd	t (84.86) = -3.59, p = 0.0005	t (8.49) = -0.1, p = 0.91
Ni	t (86.67) = 1.89, p = 0.06	t (9.95) = 0.08, p = 0.93
Rb	t (68.24) = -5.44, p = 7.534e-07	t (13) = -5.43, p = 0.0001
Sb	/	t (7.97) = 2.77, p = 0.02
Sc	t (91.16) = -7.77, p = 1.132e-11	t (10.41) = -1.31, p = 0.21
Sm	t (69.68) = -9.09, p = 1.824e-13	t (10.27) = -0.26, p = 0.79
Sr	t (72.25) = 4.75, p = 1.004e-05	t (12.21) = 0.42, p = 0.67
Ta	t (91.98) = -8.73, p = 1.048e-13	t (8.40) = -1.38, p = 0.20
Tb	t (80.75) = -9.05, p = 6.373e-14	t (12.39) = 0.47, p = 0.64
Th	t (88.73) = -10.03, p = 2.806e-16	t (8.40) = -1.26, p = 0.24
Ti	t (91.99) = -5.21, p = 1.146e-06	t (12.21) = 0.29, p = 0.77
U	t (57.14) = 3.31, p = 0.0016	t (6.89) = 1.21, p = 0.004
V	t (91.45) = 2.54, p = 0.012	t (12.67) = -1.01, p = 0.33
Yb	t (72.97) = -8.53, p = 1.378e-12	t (8.01) = -0.89, p = 0.39
Zn	t (69.26) = -4.92, p = 5.546e-06	t (10.16) = -1.05, p = 0.31
Zr	t (81.31) = -0.17, p = 0.86	t (12.98) = 0.93, p = 0.36